FINAL-REPORT
for the M.Sc.Thesis

Influence of foreshore steepness on wave velocity and acceleration at the breakwater interface

Student: N.J.Oortman

Supervisors: prof.dr.ir.M.J.F.Stive
ir.H.J.Verhagen
dr.ir.H.L.Fontijn
ir.B.Reedijk

Delft University of Technology
Faculty of Civil Engineering and Geosciences
Section of Coastal Engineering
Delft, the Netherlands

Graduation committee

prof.dr.ir.M.J.F.Stive	DUT, fac. Civil Engineering, section Coastal Engineering (chairman)
ir.H.J.Verhagen	DUT, fac. Civil Engineering, section Coastal Engineering
dr.ir.H.L.Fontijn	DUT, fac. Civil Engineering, section of Fluid Mechanics
ir.B.Reedijk	Delta Marine Consultants b.v.

Preface

In this master thesis an experimental study is described on the influence of foreshore steepness on wave velocity and acceleration at the breakwater interface. The work has been carried out within the framework of the Faculty of Civil Engineering at Delft University of Technology. The work was carried out in cooperation with Delta Marine Consultants.

I would like to thank my graduation committee, prof.dr.ir.M.J.F. Stive, ir.H.J.Verhagen, dr.ir.H.L. Fontijn and ir.B.Reedijk for their assistance and comments. I would also like to thank Delta Marine Consultants for giving me the opportunity to do this research project. Further I would like to thank dr. dipl-ing. M.Muttray for his assistance and guidance.

Finally I would like to thank the staff members of the laboratory for their help in construction of different foreshores and assistance during the experiment.

N.J.Oortman

Abstract

This Master's Thesis is a pilot research project in order to investigate which parameters, other than the wave energy density spectrum, could play a role in breakwater damage on variable foreshore steepness. The research project is based up on laboratory research, were for equal wave spectra at the toe of a coastal structure significantly more damage (order of 30%) occurs to a steep foreshore in contrast to a mild slope.

In order to investigate which parameters, other than the parameters included in the wave energy density spectrum could play a role in the increase in damage for a steep foreshore, an experiment was conducted. In the wave flume of the Fluid Mechanics Laboratory an experimental test set up was constructed. The test setup consisted of a breakwater build on variable foreshore steepnesses (1:30, 1:15 and 1:8). Tests were conducted with regular waves, were the wavelength and the wave steepness at the toe of the breakwater were kept constant per individual test. These tests were conducted for the three different foreshore steepnesses. Wave runs were completed for different wave heights and wave steepnesses. Each experiment was repeated in order to increase the accuracy.

At the breakwater the wave velocity and acceleration was measured with zero buoyant particles. The particles were monitored with a video camera. From these video images the velocity and acceleration relative to the breakwater slope were calculated.

In order to check the accuracy a reliability study of the experiment was performed. The faults in the experiment were estimated and assumed to be normal distributed. The reliability of the entire experiment was calculated for velocity and acceleration measurements.

The velocities and accelerations for up-rush and down-rush were compared for equal wave conditions and different foreshore steepnesses. The experimental data shows that the velocities for up-rush and down-rush are higher for waves travelling over a steep foreshore (order of 10%). Also the obtained accelerations for both up-rush and down-rush are higher for waves travelling over a steep foreshore.

When the wave force is calculated with a Morrison equation, the increase in force due to the increase in velocity for waves travelling over a steep foreshore is in the order of 20%. When considering that the acceleration is also larger in this case, this results an even larger total wave force.

By linking the wave force to the level of damage, it can be explained that for equal wave spectra at the toe and for variable foreshore steepness the largest damage was measured for waves travelling over a steep foreshore.

Table of contents

List of Symbols

Symbol	Definition	Unit
a	acceleration of fluid	m/s^2
A	contact area of the stones	m^2
	coefficient (Goda)	-
C_B	bulk coefficient	-
C_D	drag coefficient	-
C_M	inertia coefficient	-
d	water depth at the toe	m
D_{n50}	nominal mean diameter	m
F	force	N
g	gravitational acceleration	m/s^2
h	water depth	m
H	wave height	m
H_B	maximum wave height at the breaking point	m
H_s	significant wave height	m
H_T	wave height at the toe of the breakwater	m
k	wave number ($2\pi/L$)	-
K_D	stability coefficient	-
L	wave length	m
L_0	deep water wavelength	m
M	mass of the stone	kg
N	number of waves	-
P	permeability factor	-
r	relative error of the experiment	-
S	damage level	-
T	wave period	s
u	velocity parallel to the breakwater slope	m/s
$\overline{U}_{MAX}$	mean of the maximum measured velocity at the breakwater slope for down-rush/up-rush	m/s
V	volume of the stone	m^3
W	armour unit mass	kg

Greek symbols

α	structure slope angle	-
θ	bottom slope	-
ϕ	angle of internal friction	-
Δ	relative buoyant density of material	-
μ	mean value of the measurement error	-
ρ_s	density of stone	kg/m^3
ρ_w	density of water	kg/m^3
σ	standard deviation of the measurement error	-
ω	angular frequency of waves ($2\pi/T$)	s^{-1}
ξ	surf similarity parameter	-
ψ_{ms}	critical value Morrison-Shields	-

Chapter 1 Problem Description

1.1 General introduction

Many methods for the prediction of stability of armour units designed for wave attack have been proposed in the half past century. These design formulae have been developed, based on physical model tests. The majority of these tests have been performed with relatively deep-water wave conditions at the toe of the structure. However, in many practical circumstances coastal structures are positioned in relatively shallow water with mild or steep foreshores.

In case of coasts with steep foreshores, coastal structures suffer more damage than structures located at mild slopes. Design guidelines compensate this decrease in stability in the stability coefficients (for Hudson formula K_D-value) see Cur Report 169.

Recent laboratory research (Hovestad 2005) confirmed, that for equal deep-water waves the damage in case of a steep foreshore is larger than in case of a milder slope. Tests with identical wave spectra at the toe of the breakwater resulted in significantly more damage of the steep foreshore. Because the spectra are identical, and the damage is clearly different, this implies that damage to a breakwater on a sloping foreshore not only depends on the wave spectrum (whether at the toe of the structure or the deepwater wave spectrum). Probably there is a parameter, which is different for waves approaching over different foreshore slopes (Verhagen 2005).

1.2 Problem definition

For equal wave spectra at the toe of a coastal structure significantly more damage (order of 30%) occurs to a steep foreshore in contrast to a mild slope. Apparently the wave spectrum doesn't contain sufficient information to predict the effect of steep foreshore on breakwater armour layer stability. More insight is necessary in physical wave characteristics, which are not described by the wave spectrum, and contribute to explanation of the differences in damage.

1.3 Research objective

Wave properties that play a role in the stability of a breakwater armour unit on steep foreshores will be analysed by means of laboratory research. The objective of this Master's Thesis is to describe suitable parameters (qualitative and quantitative) that contribute to the difference in damage, and to comprise them to a foreshore steepness stability parameter. These wave parameters are other parameters than described in the wave energy density spectrum. The wave height and wave length are therefore not the parameters of interest.

The area of interest for measuring these wave variables is between the location of the incoming wave at the toe of the breakwater and the wave conditions at the breakwater interface.

1.4 Methodology

A literature study is conducted for the stability of breakwater armour units on horizontal and sloping foreshores. For the latter case a lack of knowledge was found. Therefore a study of the

physical behaviour of waves on sloping foreshores was conducted. Recent research in other fields of hydraulical engineering, with respect to the stability of non-cohesive materials, showed promising parameters. Useful information is given by Tromp (2004), Hovestad (2005) and Dessens (2004).

Experiments are needed to determine which wave parameters, other than the spectral ones, could contribute to the difference in damage. An experimental set-up was configured capable of investigating the physical processes. Three different foreshore steepnesses (1:30, 1:15 and 1:8) were tested to investigate the wave properties.

The results of the measurements are validated and analysed. From these amounts of data, the wave properties are obtained and derived. The final step is the evaluation of the different wave properties for all three foreshore slopes in addition to stone stability.

1.5 Report outline

This report is subject to describing physical wave parameters that are different for variable foreshore steepnesses. Therefore it is not in the scope of this research to perform actual damage tests. This would be favourable, however, in the current timeframe but not realistic, as these tests appeared to be very time-consuming.

Chapter 2 Theory

This chapter will note and discuss the relevant theory and design formulae for the stability of breakwaters in shallow waters. After all relevant theory is analysed the hypothesis of this master's thesis is formed. The end of this chapter will be closed with conclusions in the scope of this chapter.

2.1 Problem history

In case of coasts with a steep foreshore coastal structures suffer more damage than normally could be expected from given boundary conditions at deep water. For that reason in the CUR [1995] it is recommended to apply a heavier class of armour unit in these situations. Until recently there was no insight in the physical processes leading to this extra load. Laboratory research of Hovestad (2005) confirmed this increase of load on steep foreshores and added an interesting observation:

- Tests with identical wave spectra at the toe of the breakwater resulted in significantly (order of 30%) more damage in case of a steep foreshore, relative to a mild-sloping foreshore.

Because the spectra are identical, and the damage is clearly different, this implies that the damage to the breakwater also has to depend on a wave parameter that is not represented by the (shallow water) wave energy spectrum. Therefore it is probable that there is a governing parameter which is different for waves approaching over different foreshore slopes.

2.2 Stability formulae

Many methods for the prediction of rock-size armour units designed for wave attack have been proposed in the half past century. Common design formulae have been developed, based on physical model tests. The Hudson formula (based on Iribarren's formula) and the formulae by Van der Meer are widely known examples.

2.2.1 Iribarren

In 1938 Iribarren (d'Angremond 2001) proposed a stability formula for stones under breaking waves. As a first guess, it was assumed that the velocity in a breaking or broken wave on a slope is proportional to the wave celerity in shallow water, with the wave height as a representative measure for the water depth; $u \subset \sqrt{gH}$. Following the same reason as for stability in flow, Iribarren calculated:

$$\rho_w g H d^2 \quad \subset \quad (\rho_s - \rho_w) g d^3 \quad (\tan\phi \cos\alpha \pm sin\alpha) \qquad (2.1)$$

"drag"force resisting force slope correction

u	velocity parallel to the breakwater slope	[m/s]
g	gravitational acceleration	[m/s^2]
H	wave height	[m]
ρ_s	density of stone	[kg/m^3]
ρ_w	density of water	[kg/m^3]

d	stone diameter	[m]
ϕ	angle of internal friction	[-]
α	structure slope angle	[-]

See also figure 2.1, + and – in the slope correction are for up-rush and backwash, respectively. By raising all terms to the third power and working with the mass of the stone, the Iribarren formula is obtained:

$$M \geq \frac{\rho_s H^3}{\Delta^3 \left(\tan\phi \cos\alpha \pm \sin\alpha\right)^3} \qquad (2.2)$$

M	mass of the stone	[kg]
Δ	relative buoyant density of material	[-]

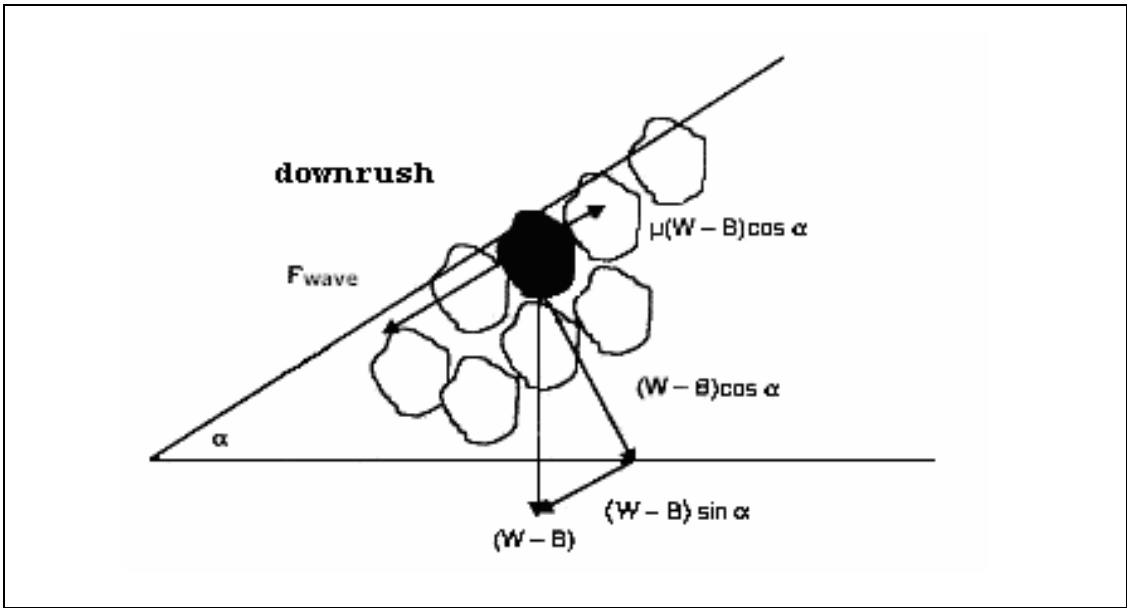

figure 2.1 Stability of rock on a slope under wave attack (down rush)

2.2.2 Hudson

Many tests were performed by Hudson in 1953 to find the constants of the Iribarren formula. For practical reasons, Hudson finally proposed another nearly similar formula (CUR Report 160):

$$W \geq \frac{\rho_s g H^3}{\Delta^3 K_D \cot\alpha} \qquad (2.3)$$

W	armour unit mass	[kg]
K_D	stability coefficient	[-]

Where K_D is a 'dustbin coefficient' taking into account stability related variables. The main advantages of the Hudson formula are its simplicity, and the wide range of armour units and configurations for which values of K_D have been derived. K_D-values are determined for; breaking or non-breaking waves, different types of armour units (interlocking/non-interlocking) and damage level. The Coastal Engineering Manual gives values for K_D for different circumstances. The formula, however, has clear limitations. The wave period is absent; this is a very important parameter, since it determines the wave steepness. The latter is of major importance to define the breaking pattern on the slope. The permeability is also not mentioned, as well as storm duration, which both has consequences for the stability.

Based on experience it is known that the effect of a steep foreshore may be expected to reduce the stability of the armour layer. Therefore where the foreshore is steeper than 1:30 the armour mass in conceptual design should be increased.

The possibility of the influence of a decrease in armour unit stability by waves travelling over a steep foreshore can thus be interpreted in the K_D-value.

2.2.3 Van der Meer

d'Angremond (2001) reports about series of extensive model tests, which were conducted by Van der Meer in 1988. The tests included structures with a wide range of core/underlayer permeability and a wide range of wave conditions. Van der Meer (1988) based his analysis on a large data set, of which most tests concerned conditions with relatively deep water at the toe. Based on a relatively small amount of tests it was proposed to use the wave height $H_{2\%}$ (the wave height exceeded by 2% of the waves) so that the deviation from the Rayleigh wave height distribution, described by the factor 1.4 $/ (H_{2\%} / H_s)$, was included in the formulae. Two formulae were derived for plunging and surging waves, respectively:

$$\frac{H_s}{\Delta D_{n50}} = 6.2 P^{0.18} \left(\frac{S}{\sqrt{N}} \right)^{0.2} \xi^{-0.5} \qquad \text{plunging waves } \xi < \xi_{transition} \qquad (2.4)$$

$$\frac{H_s}{\Delta D_{n50}} = 1.0^{-0.13} \left(\frac{S}{\sqrt{N}} \right)^{0.2} \sqrt{\cot \alpha} \cdot \xi^{p} \qquad \text{surging waves } \xi > \xi_{transition} \qquad (2.5)$$

The transition from plunging to surging waves can be calculated using a critical value:

$$\xi_{transition} = \left[6.2 P^{0.31} \sqrt{\tan \alpha} \right]^{\frac{1}{P+0.5}} \qquad (2.6)$$

H_s	significant wave height	[m]
D_{n50}	nominal mean diameter	[m]
P	permeability factor	[-]
S	damage level	[-]
N	number of waves	[-]
ξ	Surf similarity parameter	[-]

The formulae of Van der Meer are a step forward compared to Hudson's equation, because more relevant parameters are included, like the Iribarren number (and thus the wave steepness), porosity of the structure, damage level and the number of waves. The physical base of Van der Meer equations is in case of steep and shallow foreshores still weak, since the majority of these

tests have been performed with relatively deep-water wave conditions at the toe of the structure. In many practical circumstances coastal structures are positioned in relatively shallow water. So it can be concluded that the use of the Van der Meer formulae is not well validated for shallow water conditions and relatively mild or steep sloping foreshores.

2.2.4 Van Gent

Van Gent (2003) studied the stability of rock slopes with shallow foreshores, such that wave breaking occurs on the foreshore before the waves reach the structure. Data sets with 1:100 and 1:30 foreshores (207 tests) were combined and analysed to obtain more generic recommendations about how to deal with situations with shallow foreshores. The data obtained from the physical model tests were used to analyse how the formulae by Van der Meer (1988) can be applied or modified for applications including conditions with shallow foreshores.

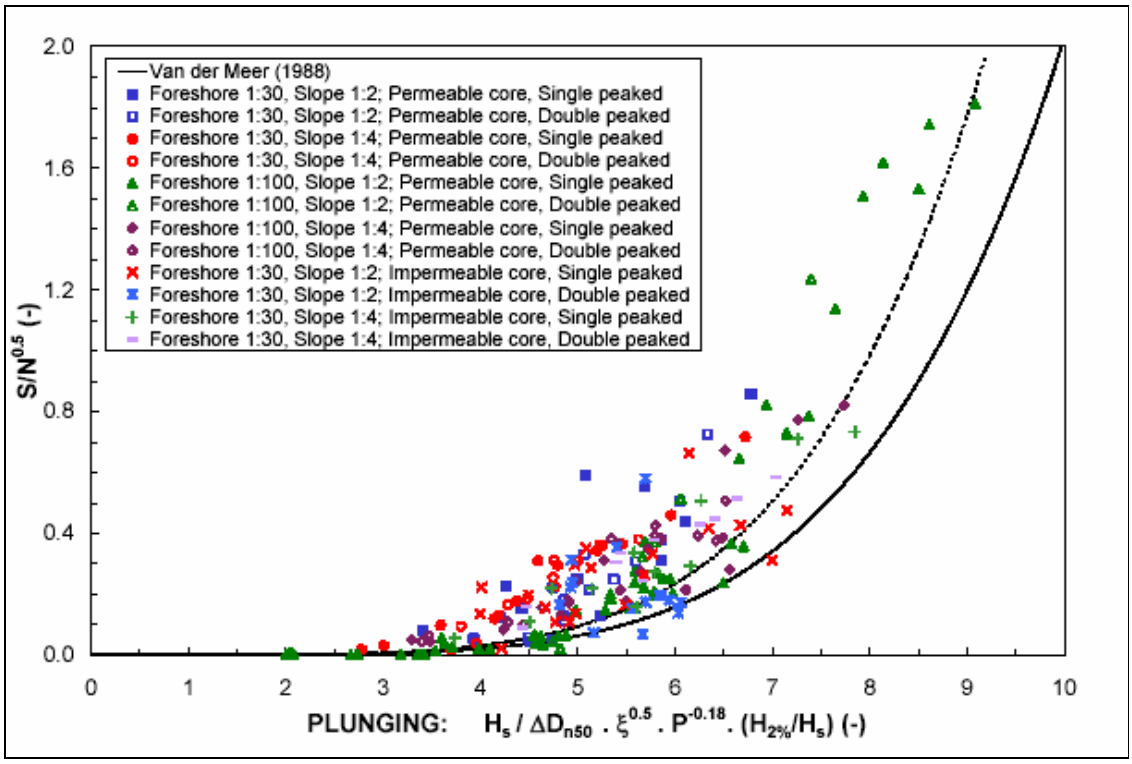

figure 2.2 Data Van Gent, with shallow foreshore compared to Van Der Meer formula with 5% confidence level (2003).

The new data showed a clear difference in stability, compared with the Van der Meer formulae. See figure 2.2 for plunging waves.

Replacing the ratio $H_{2\%}/H_s$ by 1.4 showed that using this approach the data is closer to the prediction formula, but that the differences are still large. Therefore, it was analysed whether the wave period T_m could better be replaced by another wave period. For this purpose not only the wave period was replaced by several other wave periods, but for each wave period the coefficients from the Van der Meer formulae were re-calibrated, as illustrated in figure 2.3.

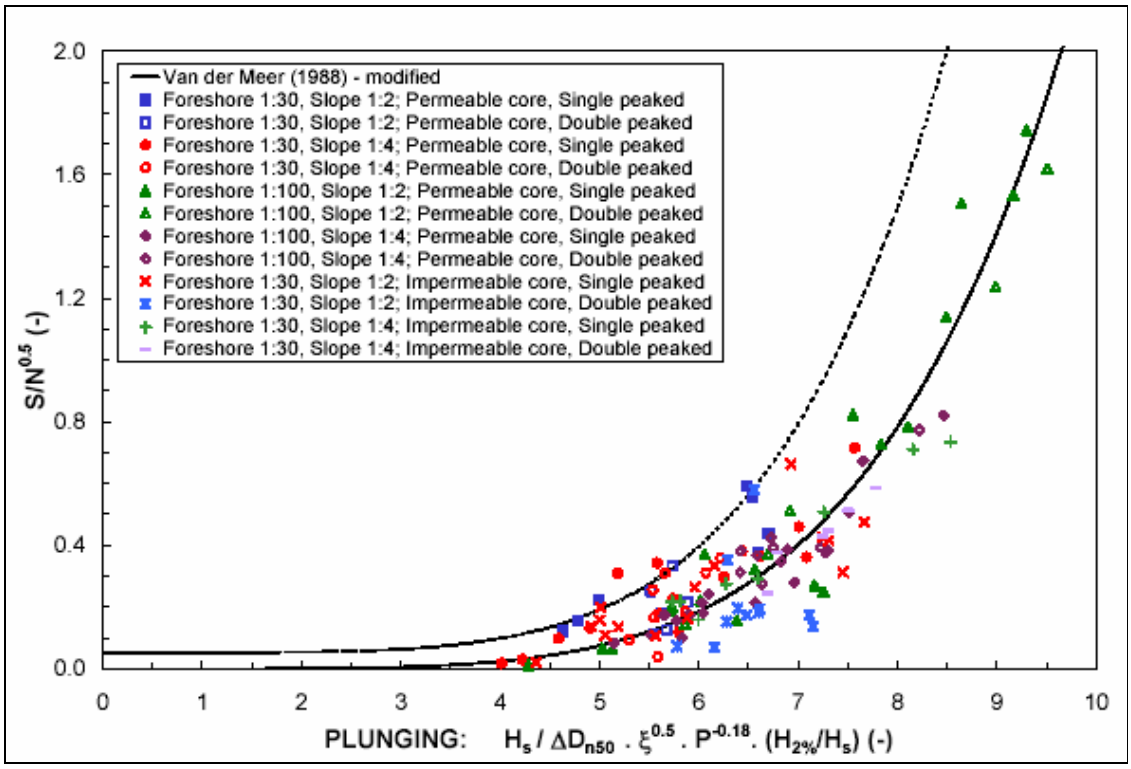

figure 2.3 Data compared to a modified formula from Van der Meer (1988) (plunging waves), re-calibrated and with the wave period $T_{m-1.0}$, and with a 5% confidence level.

Van Gent concludes that for applications with shallow foreshores the current Van der Meer formulae (1988) can better be applied by using the spectral wave period $T_{m-1.0}$ instead of the mean wave period T_m, by re-calibrating the coefficients and by adapting the confidence levels.

It is interesting to see that Van Gent includes the effect of a shallow foreshore on the stability of the armour unit. Although he argues that the use of another spectral wave period satisfies to define the stability of an armour unit in shallow (mild sloping) foreshores, no conclusions are drawn on differences in armour stability due to foreshore steepness.

2.2.5 Goda

Goda (1985) includes the effect of the steepness of the foreshore on the increase of the limiting breaker height. The formula is based on tests with regular waves and applied to random waves, with a model of random wave breaking. A design diagram is given in figure 2.4. The breaker height is a function of the foreshore steepness, the local water depth (of interest) and the deep water wavelength. The formula is given as follows:

$$\frac{H_B}{L_0} = A\left\{1-\exp\left[-1.5\frac{\pi h}{L_0}\left(1+15\tan^{\frac{3}{3}}\theta\right)\right]\right\} \qquad (2.7)$$

H_B	Maximum wave height at the breaking point		[m]
A	coefficient:	0.17 for regular waves	[-]
		0.12 random waves lower breaking limit	[-]
		0.18 random waves upper breaking limit	[-]

θ	Bottom slope	[-]
h	water depth	[m]
L_0	deep water wavelength	[m]

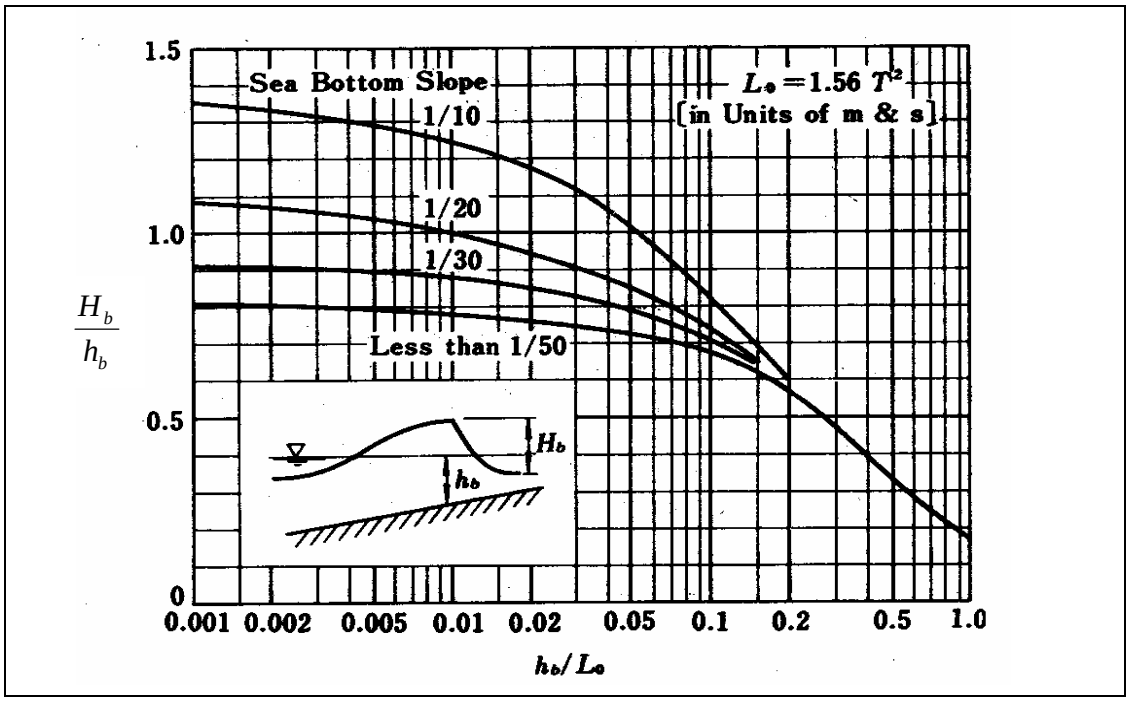

figure 2.4 Design diagram for limiting breaker height of regular waves, Goda (1985).

Example:
By simulating a simple realistic case, with a deep water wavelength of 100m a water depth of 10m at the toe of the breakwater, and a variable foreshore steepness, of 1:50, and 1:15 the following breaker heights are respectively obtained (A=0.18); 7.2m and 8.7m.

This means an increase of 17% in wave height. By filling in these breaker heights in the Hudson formula, this results in a increase in stone weight of 43% (wave height in stability formula is to the third power).

With the observations of Goda it is possible to define a difference in breaker heights for steep foreshores. This can explain a difference in damage for variable foreshore steepnesses with the same deep water wave conditions.

The observations of Goda, however do not give a reason why differences in damage are possible for an variable foreshore steepness and equal wave energy density spectrum at shallow water, e.g. location of the toe of an breakwater.

2.3 Foreshore steepness and armour unit stability

Hovestad (2005) showed a significant difference in damage for variable foreshore steepness and an equal wave energy spectrum at the toe of the breakwater. The research was carried out in the Research Flume in the Fluid Mechanics Laboratory at Delft University of Technology.

The breakwater was built on a 1:8 and a 1:30 foreshore. These slopes were selected to be able to clearly observe the difference in foreshore-slope effect on armour unit stability.

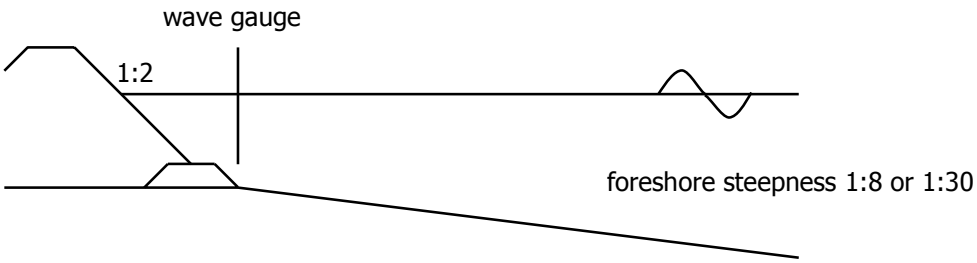

figure 2.5 Experimental set-up Hovestad (2004).

Experiments with similar wave energy spectra at the wave board
During tests with equal wave energy spectra at the location of the wave board, tests showed that damage to the breakwater was up to 64% higher on the 1:8 foreshore compared to the 1:30 foreshore. This difference in damage can be explained by larger breaker heights near the toe due to the steep foreshore. Apparently the waves could shoal until a larger wave height before breaking at the steep foreshore. As showed with the theory of Goda a larger breaker height can occur on a steep slope.

Experiments with similar wave energy spectra at the toe
In these tests wave energy spectra at the toe of the breakwater were matched. The results of the research show that even if the wave conditions at the toe of the breakwater are almost similar in the steep and the mild-foreshore case, the damage to the breakwater can still be about 30% higher for the steep foreshore.

This latter case resulted in the important statement:
Because the spectra are identical and the damage is clearly not identical, this implies that damage to the breakwater also has to depend on a wave parameter, which is not represented by the shallow water wave energy spectrum, and it has to be a parameter that is different for waves approaching over different foreshore slopes.

2.4 Influence of velocity and acceleration of flow on stone stability

The actual design formulae for the stability of stone do not contribute to the research objective. However it is known that the velocity has an important influence on the stability of stone. Research by Dessens in 2004 showed that next to the influence of velocity, the acceleration is another parameter which has an effect on stone stability in stationary flow. It is interesting to

mention these observations. Tromp investigated whether the acceleration is also of influence on stone stability in oscillating conditions.

2.4.1 Tests on stone stability in acceleration of stationary flow

Dessens (2004) conducted laboratory research on the influence of flow acceleration on stone stability. Experiments were set up with stationary flow. In a research flume a tapering was constructed. Because of this tapering the flow was accelerated. By keeping the decrease in width constant, and by varying the length of the tapering per test, the velocity in the tapering was kept equal, but resulted in different accelerations for each test (see figure 2.6). For each combination of velocity and acceleration the critical condition for moving stones was determined.

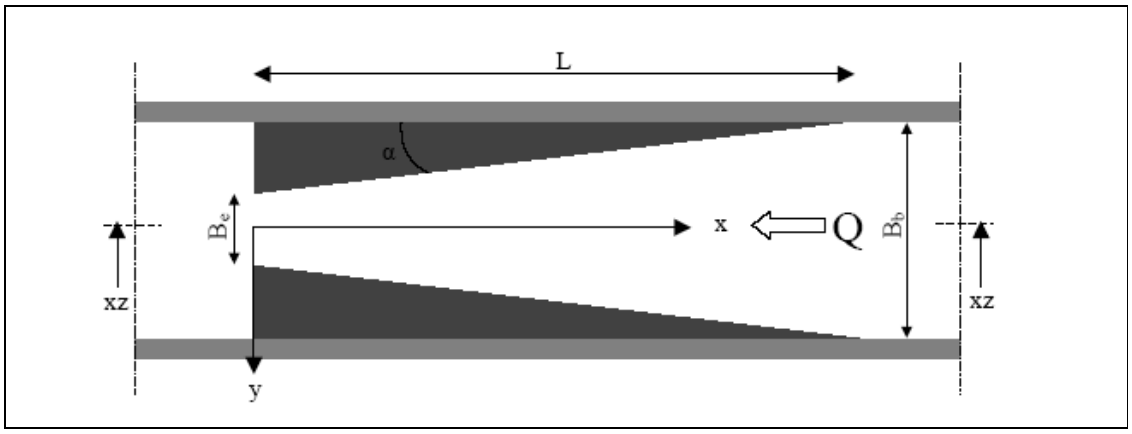

figure 2.6 Top view of tapering in research flume, Dessens (2004).

The test showed that for a given stone size the critical velocity decreased with an increase of the acceleration. To describe this, a stability parameter has been developed on the basis of the Shields parameter, but including the acceleration in the same style as is used in the Morrison equation. The dimensionless Morrison-Shields equation notes:

$$\psi_{ms} = \frac{\frac{1}{2} C_B \rho d^2 u^2 + C_M \rho d^3 a}{\rho \Delta g d^3} = \frac{\frac{1}{2} C_B u^2 + C_M d a}{\Delta g d} \qquad (2.8)$$

ψ_{ms}	Critical value Morrison-Shields	[-]
C_B	bulk coefficient	[-]
C_M	inertia coefficient	[-]
a	acceleration of fluid	[m/s^2]

The formula shows the additional effect of acceleration next to the velocity on particle movement. This result explained the idea that stability of stone was not only a function of the velocity.

2.4.2 Stone stability in acceleration by waves in shallow water

Tromp (2004) performed laboratory research on the influence of fluid velocity and accelerations on the threshold of motion under waves. The threshold of motion by waves was investigated in shallow water on a sloping foreshore. Tests were conducted in a research flume with regular

waves with 1:30 foreshore steepness. The hydraulic stability of non-cohesive sediments was investigated as a function of near-bed orbital velocity and acceleration.

As was expected, at deep water the phase shift between velocity and acceleration is in the order of $\pi/2$, which makes that the effect of acceleration can be neglected. But in a shoaling wave, the time interval of maximum velocity and maximum acceleration becomes smaller. This decrease in phase shift is indicated and shown in figure 2.7. At the same time the value of the acceleration is increasing relatively to the increase in the maximum velocity.

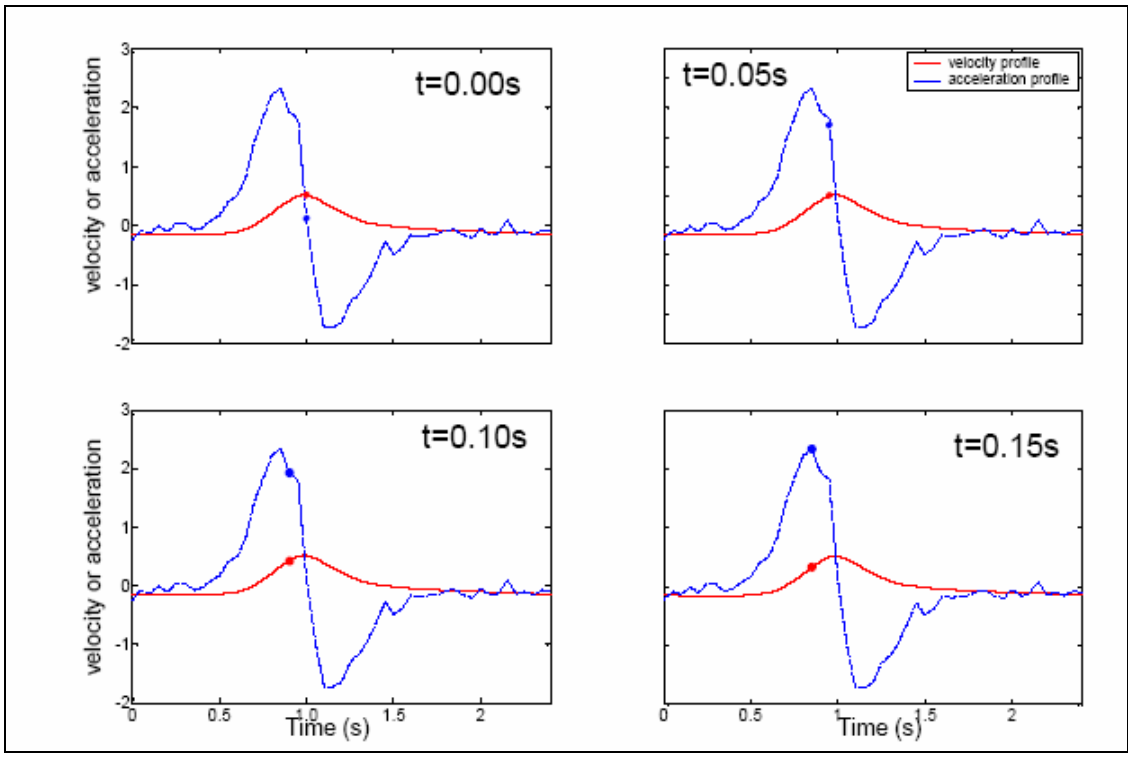

figure 2.7 Instantantaneous values of near-bed horizontal velocities and accelerations for a wave with H_0=12.5cm, h_0=55 cm, T=2.5s and X=18.68m. The red line represents the near-bed orbital velocity and the blue line the near-bed orbital acceleration. The time in the upper right frame of the plots represents the time before passage of the wave crest. (Tromp 2004).

Movement of stones was monitored with a video camera. Stone movement and the values of velocity and acceleration are coupled to show the influence. The picture shows that maximum near-bed velocity occurs at the maximum surface elevation. And that both the velocities and the accelerations have large positive values at the time stones starts to move. The other videos showed the same (see figure 2.8).

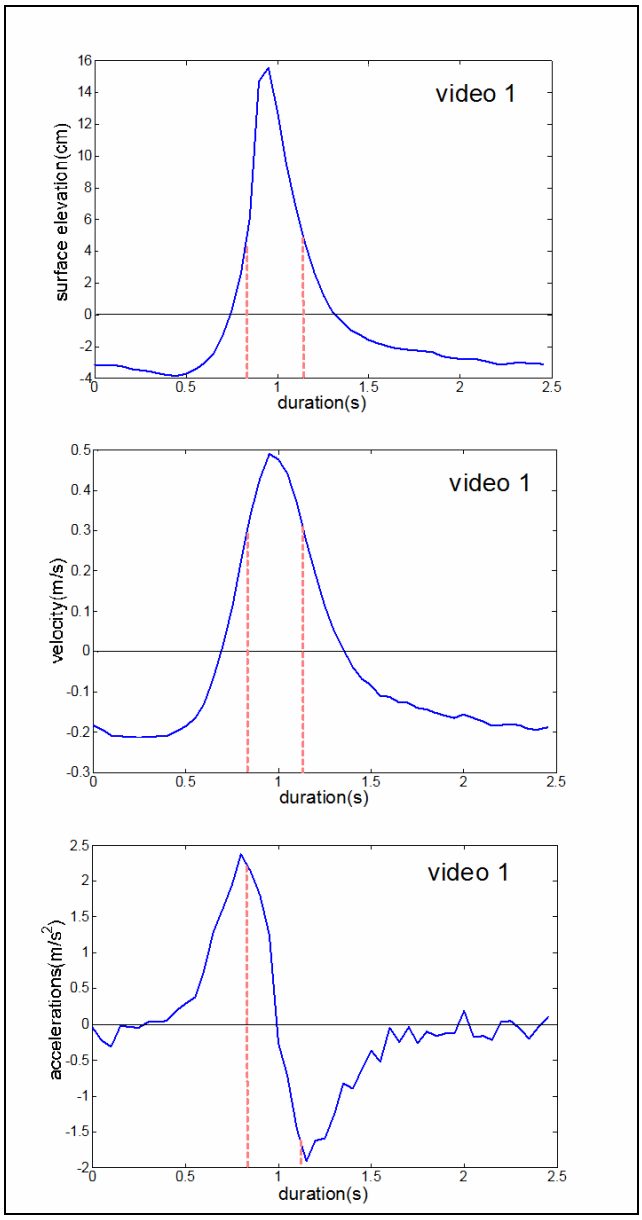

figure 2.8 graphical representation of the start and ending of stone movement as a function of surface elevation, the horizontal near –bed velocity and acceleration, Tromp (2004).

During the tests Tromp made detailed video observations of stone movement. The movements could be correlated to the observed near bed velocity and near bed acceleration. This indicates that also for an oscillatory motion a Morrison-type of approach seems valid. Situations were created with nearly similar near bed velocities, but with different accelerations. When using these velocities and accelerations in a Morrison-type of equation it proofs that the threshold of motion is dependent on both the horizontal near-bed velocities and the acceleration.

2.5 Model that includes acceleration and velocity

In a wave field velocity forces and acceleration forces are present. The consideration of using the influence of these parameters in a stability formula for breakwater armour units is not applied. However, Morrison developed a formula for the stability of bed material under waves, which takes both velocity and acceleration into account. Morrison proposed a formula for this wave force, which is the sum of drag force and pressure force.

$$F_{wave} = F_{drag} + F_{acceleration} = \frac{1}{2} C_D \rho A u|u| + C_M \rho V \frac{Du}{Dt} \qquad (2.9)$$

F	force	[N]
C_D	drag coefficient	[-]
A	contact area of the stones	[m^2]
V	volume of the stone	[m^3]

The drag term is generated by the fluid velocity and the fluid accelerations form horizontal acting pressures around an object. Since, next to a drag force, also a lift force and other turbulent forces act on a particle, the Morrison formula can be rewritten as (Tromp 2004):

$$F_{wave} = F_{bulk} + F_{acceleration} = \frac{1}{2} C_B \rho A u|u| + C_M \rho V \frac{Du}{Dt} \qquad (2.10)$$

The influence of drag, lift and turbulent forces are processed in a bulk coefficient C_B. The calibration of the two coefficients is of major concern, when applying this formula.

2.6 Relation to breakwater stability and foreshore steepness

In the present stability equations the load parameter is a function of the energy density spectrum at the toe of the construction. An energy density spectrum does not contain any information on the phase shift. Also the energy density spectrum does not contain any information on wave asymmetry. Therefore the present stability equations cannot distinguish between waves which have at the toe of the structure an identical energy density spectrum, but a difference in phase angle between velocity and acceleration. This phase angle depends, amongst others on the slope of the foreshore.

Because of higher order effects the wave crests become steeper and the wave troughs become flatter. This increases the velocity and acceleration considerably. The wave steepness, defined as the ratio between wave height and wave length does not change. But when the steepness of only the part above the still water line is considered, this steepness increases considerably.

From the tests of Tromp follows that for a given velocity, the stability decreases because of the effect of acceleration.

2.7 Hypothesis

The hypothesis of this research project is that the velocity and the acceleration of the fluid motion are of influence on the stability of breakwater armour units under wave conditions on sloping foreshores. Due to the sloping foreshore the wave profile becomes more peaked, resulting in a phase shift (other than 90°) between velocity and acceleration. At the moment of maximum velocity the acceleration is still zero, however the acceleration can have a contribution to the velocity, close to the maximum value. Therefore the acceleration can have an influence on the reduction of stone stability. Since the waves travel over a different foreshore, probably there exists a difference in wave form. Due to the difference in peakedness, the velocity and acceleration values can quantitative differ, as can the phase shift between velocity and acceleration differ, for variable foreshore steepness.

Since most damage occurred at the steepest foreshore it is assumed that the increase in velocity and acceleration will be largest at the 1:8 foreshore and lowest for the 1:30.

2.8 Conclusion

Actual design formulae for the stability of breakwaters do not take the foreshore steepness into account. Only wave-related parameters are used, e.g. (spectral) wave height, period, storm duration and parameters related to the structure, e.g. permeability, slope of structure, damage level, type and density of the armour unit. Van Gent concludes that the Van der Meer formulae underestimate the stability of rock on shallow foreshores.

Tromp showed that in case of wave conditions also a Morrison equation is valid. Due to a sloping foreshore, the wave profile becomes more peaked. Tromp showed that this peakedness results in a phase shift (other than 90°) of the velocity and acceleration and to a relative increase of acceleration. The acceleration contributes to a decreasing stability of bottom material under wave conditions, and should be accounted for, next to the orbital velocity.

The peakedness of the waves is not included in stone stability formulae under wave conditions. Neither is the influence of acceleration and velocity mentioned in any design formulae. Since the wave energy spectrum does not include any phase information, it is not possible to reconstruct the actual wave conditions. The information about the peakedness of the waves is lost, and so is the acceleration and velocity information.

The velocity and acceleration information, as the peakedness of the waves, seem to be important parameters in breakwater stability.

Chapter 3 The experiment

This chapter deals with the physical model test that was conducted to determine differences in velocity and acceleration in waves, shoaling at variable foreshore steepness.

3.1 Introduction experimental set-up

The objective of this research is to investigate physical wave properties that are different in shallow water at variable foreshore steepness, other than the spectral energy density spectrum. The point of interest for the variables is at the toe of the breakwater. Since the wave height and wave period (and thus wave length and steepness) are described in the spectrum, these variables are constant. In this experiment they will also be kept constant per individual test.

The differences in particle velocity and acceleration, due to a difference in peakedness of the waves are investigated at the face of the breakwater, e.g. where the damage should occur. In order to create the biggest possible difference in peakedness (if any), a range of foreshore slope steepness was selected, as different as possible.

The peakedness of a wave and its influence on the acceleration and velocity is best to analyze for simple regular waves. In this case the wave height and length can be kept constant and results for different foreshores are relative simple to compare. Since particle velocity and acceleration depend on the wave steepness and the water depth, these are kept constant per experiment. To keep the relation with a wave spectrum also experiments are conducted with bichromatic waves.

It is not in the scope of this research project to do actual damage tests, the armour layer of the breakwater will therefore be fixed.

3.2 Facilities and equipment

This paragraph gives a technical description of the used facilities and equipment necessary to execute the experiment.

3.2.1 Wave flume and generator

Physical model tests were performed in the research flume "Lange Speurwerkgoot" at the Fluid Mechanics Laboratory of the Faculty of Civil Engineering and Geosciences at Delft University of Technology.

This wave flume has an effective length of 42m, a width of 80cm and a height of 1.0m. The facility is equipped with a wave board for generating regular/monochromatic and irregular/random waves in relatively shallow water by a translatory wave board with a two-metre stroke, active reflection compensation (ARC) and a second-order wave generation technique. This means that the second-order effects of the first higher and first lower harmonics of the wave field are taken into account in the wave board motion. The water level in the flume is adjustable by an inlet and outlet system.

On the bottom of the flume a semi-permanent concrete slope with a 1:30 concrete foreshore was constructed. The starting point of the slope is located at 8.70m from the central position of the

wave board, see figure 3.1. The flume dimensions are of great importance to the experimental set-up, as will be outlined in the next section.

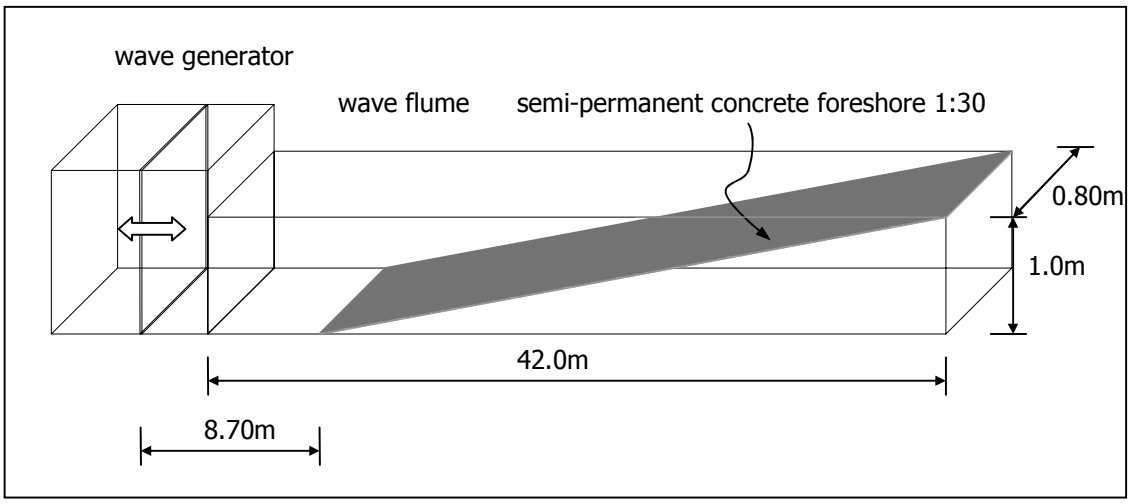

figure 3.1 dimensions of wave flume.

3.2.2 Foreshore steepness

In total, three different foreshore steepnesses are being used. As already mentioned, the flume is equipped with a concrete slope with a 1:30 inclination. Since it is a large effort to install or to remove such a foreshore, it's kept in place and treated as the mildest steepness possible in this experiment.

The choice of the steepest foreshore to be used is largely a practical consideration. Due to a total height of the flume of one meter, one has to regard the construction height of the breakwater and the water depth of the toe (20cm): the steepest possible bottom is then 1:8. In this case the length of the foreshore is in the order of one or two times (the largest) wavelengths. This is necessary in order to get a good shoaling wave, which adapts to the bottom profile. Finally a third steepness was chosen between the steepest and the mildest possible foreshore, resulting in a 1:15 slope.

By using multiple foreshore steepness, it is perhaps possible to see a pattern in the results of the data, which can explain the problem definition.

Due to the fixed 1:30 concrete slope, the position of the breakwater varied due to the different foreshore steepness, as illustrated in figure 3.2.

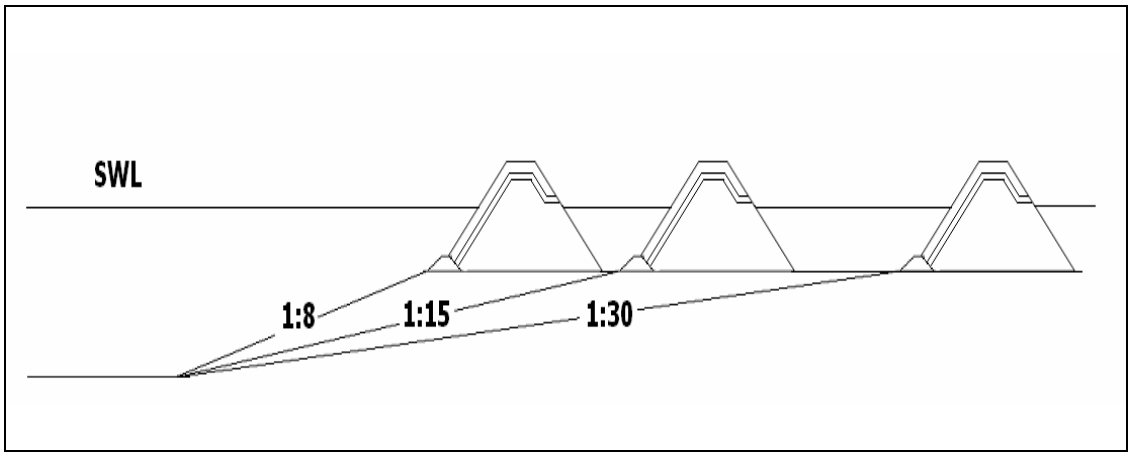

figure 3.2 Different foreshore steepness and position of the breakwater in the flume (not to scale).

3.3 Measuring instruments

To conduct a successful experiment, the choice and location of the proper instruments is very important. The choice of instruments depends on a number of aspects to be regarded (American Society of Civil Engineers 2000).

Which physical parameters must be measured to make a meaningful interpretation of the physical process?

- The physical parameters of interest. These parameters can be divided in two categories; independent and dependant variables.
- At which locations should the measurements be taken?
- Which instruments are suitable and available for the experiment?
- Which is the required accuracy and what is the reliability of the experiment?
- Which instruments are available?

Each of these important questions will be treated in the next paragraph.

3.3.1 Independent variables

The experiment has a couple of independent physical variables which can be varied, to get different results in the outcome of the experiment. To obtain different velocity and acceleration profiles a couple of parameters are varied throughout the experiment; these are the independent variables. Four different independent variables are present:

- Wave height
- Wave period
- Wave phase
- Foreshore steepness

By varying the wave height and wave period different wave steepnesses are obtained. This ratio is off influence on the orbital velocity and acceleration. One can imagine that a short period and a large wave height will give a larger velocity, compared to a large wave period and short wave height. Therefore it is not necessary to vary the water depth.

By varying the wave phase in two different values it is possible to obtain bichromatic waves. This type of wave will be used in the experiment, next to regular/monochromatic waves. See paragraph 3.4.1 for more details about the wave conditions in the experiment.

In the hypothesis it is assumed that the foreshore steepness is of influence on the velocity and acceleration profile. In total three different foreshore steepnesses will be treated a 1:30, 1:15 and a 1:8 slope.

3.3.2 Dependent variables

The dependent variables are variables which can be derived, or are obtained from the output of the independent variables. They are:

- Wave length
- Particle displacement
- Particle velocity
- Particle acceleration

The wave length is calculated with the dispersion relation, well known from the linear wave theory. However some remarks must be made, since the theory is valid for linear waves over a flat bed. Regular waves are indeed used, however since they travel over a sloping bed they become non-linear and therefore the theory is not completely valid, but still applicable.

$$\omega^2 = gk\tanh(kh) = g\frac{2\pi}{L}\tanh(\frac{2\pi}{L}h) \qquad (3.1)$$

ω	angular frequency of waves ($2\pi/T$)	(s^{-1})
L	wave length	(m)
k	wave number ($2\pi/L$)	(-)
h	water depth	(m)

The fluid velocity and acceleration is derived by differentiating the particle displacements in time, see figure 3.3. The particle displacement at the interface of the breakwater is a function of the wave profile; the wave height, wave length and probably the skewness of the wave.

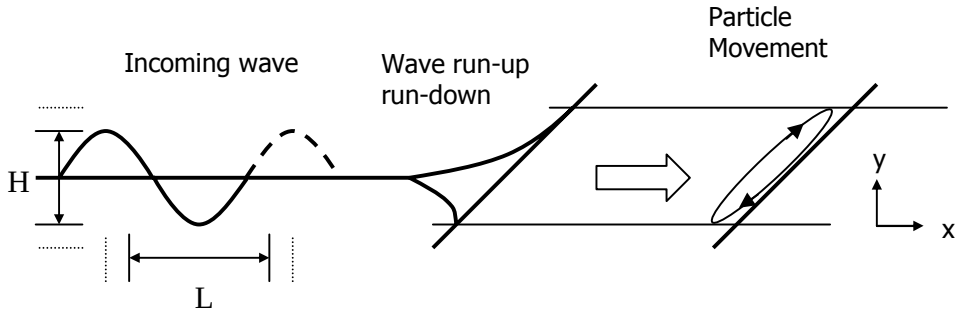

figure 3.3 Incoming wave and particle movement

3.3.3 Location of measurements

The geometrical measurements can be done in advance of each series of tests. The foreshore and the breakwater are installed. The still water level for each experiment is the same, e.g. 20cm

water depth at the toe of the construction, which coincides with a water depth at the wave board of 70cm.

Wave conditions are measured at three different locations; at the toe of the breakwater, at he wave board and halfway the foreshore construction. In this case a good visualization of the development of the shoaling wave, e.g. wave profile, is obtained.

Measurement of the fluid velocity and acceleration of the wave is measured at the interface of the breakwater, since this interface is the location where damage occurs.

3.3.4 Choice of instruments

The choice of instruments depends on which instruments are suited for the experiment and above all, which instruments are available.

The wave height and wave period is measured with three sets of 50 Hz analogue wave gauges. This frequency is enough to describe an accurate wave profile. Each set consist of two wave gauges. In this setup it is possible to separate the reflected wave from the signal, and thereby calculating the incoming wave.

A more or less standard procedure for measurement of velocity and acceleration is done with a 50 HZ electro magnetic current meter (EMS). The use of this instrument at the interface of the breakwater was in this experiment not possible, due to the setup of the experiment. The EMS did not remain under (sufficient) water, and metal objects were close to the apparatus. These and other factors made the interpretation of measurements with an EMS measurement unreliable.

Another measuring method was conducted by monitoring the particle image displacement. The water movement of waves is monitored with a video camera (25 HZ) by zero buoyant (as possible) particles. From this videotape the particle movement is analysed (frame by frame) and converted from pixel scale to the international system of units. From the particle displacement profile it is possible to calculate particle velocity and acceleration. By separating each frame a higher (50 HZ) sampling rate was obtained.

3.3.5 Accuracy and reliability

Quantifying measurement errors is very important in order to establish the reliability of the experiment. The relative error of these parameters can be derived from the error in the measured variables. Relevant measuring errors and their magnitude are tabulated below.

Measurement errors are divided into two categories; experimental and transformation errors. The first category was made during the actual test in the flume. The second category contains errors that arise during the data processing.

Experiment in flume:
The wave height, wave period and water depth contain errors due to instrumentation inaccuracy. Particle inertia (due to a difference in density) accounts for the error that the particle does not exactly follow the wave profile. At maximum run-up it "shoots" further up the breakwater, vice versa with down rush.

Transformation and software:
The reflected wave is separated from the wave signal. The first harmonic is used only. Higher harmonic components and free or bound harmonics are not taken into account. Tests were performed to check the accuracy (and validity) of the software package for separating the

reflected and incoming wave from the wave signal. Tests were conducted on a slope with breakwater and without breakwater. In the latter case the waves break on a 1:30 slope, whereas wave reflection is neglectible.

Particle tracing also contains errors. With the package (MultiscanXY) particles were traced. Converted video footage and data output show deviations due to not exact tracing of the particles. Another aspect of flaws in the experiment is the breaking of light rays in the transition of water to air (deviation due to the glass wall is neglectible). For small angles this breaking of light is a constant with the magnitude of 1.33 and therefore not mentioned in the analysis.

The wavelength is calculated from the wave record (wave elevation as a function of time). Since the wave celerity is not recorded, the wavelength is calculated with the linear dispersion relation. This relation is only valid for a flat bottom. General acceptance seems possible for very mild slopes like the 1:30 case. Serious deviations are accounted for the steep 1:8 bed slope.

The variable of interest is the displacement parallel to the breakwater as a function of time. From this variable the velocity and acceleration can be calculated. The displacement of the particles (in reference plane x and y see figure above) is monitored at the breakwater and is a function of wave height and wavelength. Errors made in the experiment, to analyze the particle movement, are given in table 3.1 and are represented by notion a until f. The velocity and acceleration is a function of the displacement and therefore also represented by notion a until f.

Variable	Instrument	Absolute Error	Av. low Value	Relative error
Experiment in flume				
a) wave height	wave gauge	0.01cm	1.0cm	1.0%
b) wave period	wave gauge	0.01s	1.0s	1.0%
c) particle position	Camera	0.1 cm	2.0cm	5.0%
Transformation & Software				
d) incoming wave height	1st order wave refl.	0.5 cm	6.0 cm	8.3%
e) particle tracing	Camera	1.0 cm	13.3 cm	7.5%
f) wave length	Lin. dispersion relation	7.0 cm	133 cm	5.0%

table 3.1 Relative errors per variable

3.4 Physical model test

Physical model tests were conducted, first the wave conditions are treated, next the used breakwater model and finally the setup of the model test.

3.4.1 Wave conditions

To check the influence of acceleration and velocity over different slopes, regular waves and bichromatic waves are used. Different velocity and acceleration profiles can be obtained using constant water level and by varying the wave height and wave steepness.

Regular waves are used, because this would indicate that for each individual test the velocity and acceleration pattern should be the same. Differences in velocity and acceleration can still vary due to a deviation in the peakedness of the wave. Also all phase information is present. By using a wave spectrum all phase information is lost. That includes that an actual reconstruction of the wave record is impossible.

Bichromatic waves are used to keep the wave pattern simple and thus the velocity and acceleration pattern. By using bichromatic waves it is still possible to make a relation to a wave energy density spectrum.

A ratio of wave height over wave length of 6% is at sea conditions regarded as the maximum steepness. Therefore in this experiment it is also the maximum steepness. The lowest steepness will account 2%. Wave heights at the toe of the structure are ranging from 6cm till 12cm (see table 3.1).

S_T	H_T	L_T	H_T	L_T	H_T	L_T	H_T	L_T
0,03	0,06	2,00	0,08	2,67	0,10	3,33	0,12	4,00
0,04	0,06	1,50	0,08	2,00	0,10	2,50	0,12	3,00
0.06	0.06	1.00	0.08	1.33	0.10	1.67	0.12	2.00

table 3.2 Wave heights and wave steepness at the toe of the breakwater

Breaking waves are not taken into account, since it is not possible with the available equipment to monitor the particle displacements under these circumstances. Therefore only surging waves are treated.

In advance the breaker depth is calculated by the method of Shuto, reported in Goda (1985). Shuto regards a breaker depth, dependant on foreshore steepness. Breaking on the foreshore of 1:30 is most probable to happen (spilling breakers), therefore a water depth of 20cm is checked. The method uses the ratio of water depth over the deep water wavelength. Using this method a breaker depth of 16cm would occur for largest deep water wavelength. A water depth of 20cm is sufficient.

Bichromatic waves are obtained by using the same first harmonic period as used with regular waves. The second harmonic wave period is built with an 0.05 s difference. The wave heights of the first and second harmonic are equal to the half of the regular wave height, so the maximum wave height is equal to the wave height of the regular wave. In figure 3.4 a bichromatic wave with a (maximum) wave height of 12cm is illustrated.

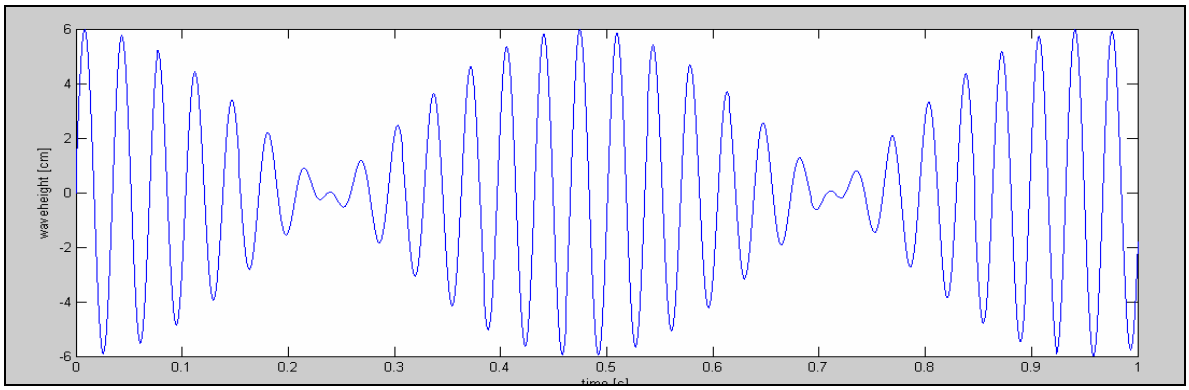

figure 3.4 Bichromatic wave

During the experiment a wave length of 4 meters induced a software error. The wave length becomes to large, and the decomposition software could not calculate the incoming wave. A wavelength of one meter or shorter was also impossible, the wave period becomes to short, which causes spurious waves (and a failing wave board).

For regular waves and bichromatic waves 10 different wave scenarios are possible. Keeping in mind the three different foreshore slopes, 60 different scenarios are being evaluated.

	tan β	S_{toe}	H_{toe} [cm]	regular waves	Bichromatic waves
A	1 : 8	0,03	6/8/10/12	x	
		0,04	6/8/10/12	x	
		0,06	6/8/10/12	x	
B	1 : 8	0,03	6/8/10/12		x
		0,04	6/8/10/12		x
		0,06	6/8/10/12		x
C	1 : 30	0,03	6/8/10/12	x	
		0,04	6/8/10/12	x	
		0,06	6/8/10/12	x	
D	1 : 30	0,03	6/8/10/12		x
		0,04	6/8/10/12		x
		0,06	6/8/10/12		x
E	1 : 15	0,03	6/8/10/12	x	
		0,04	6/8/10/12	x	
		0,06	6/8/10/12	x	
F	1 : 15	0,03	6/8/10/12		x
		0,04	6/8/10/12		x
		0,06	6/8/10/12		x

table 3.3 Used wave conditions and foreshore steepness

3.4.2 Breakwater

The breakwater is constructed as a simple trapezoidal rubble mound breakwater. The seaward side of the breakwater has a 1:2 slope and the backside has a 1.1.5 slope. The total height of the breakwater is 45cm and has a water depth at the toe of the construction of 20cm. The rock has a D_{n50} of 1.57cm and a specific density of 2790 kg/m^3.The riprap armour will be fixed to the construction by a thin wire netting, where the meshes will be just small enough to entrap the armour layer. In this way the influence of the wire will be of minor influence on the structures porosity and roughness. The crest of the breakwater was at a level such that no overtopping occurred. See also figure 3.5 and figure 3.6.

Scaling of stones for laboratory research is always a bit difficult, as scaling problems may arise. The Reynolds scaling criterion states (in a simple manner) that the Reynolds number should remain large enough to keep turbulence. In the case of applying quarry run and applying the filter rules from the CUR the core material becomes so fine, that flow in the core becomes viscous. This changes the hydraulic conditions of the core dramatically. An easy solution is to make the core material larger. Burchart et al. (1999) have proposed a theory for scaling the core material in breakwaters. Using this method a stone diameter close to the diameter of the armour layer was found. Since the properties do not have to match exactly a real life breakwater, the same diameter of the armour layer is chosen. This makes the use of a filter redundant, however for inspection of the integrity of the breakwater a contrasting coloured filter layer is applied.

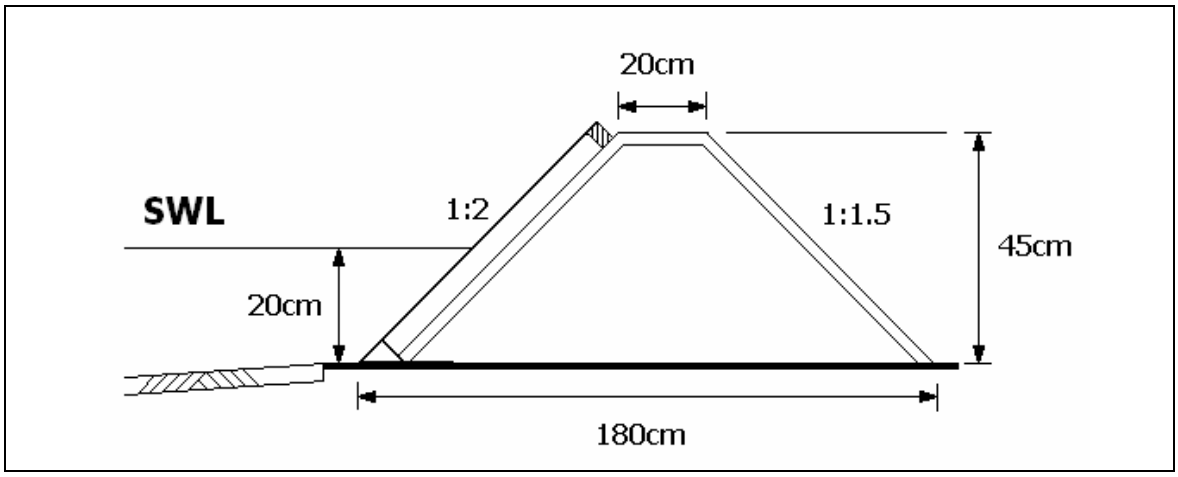

figure 3.5 dimensions breakwater

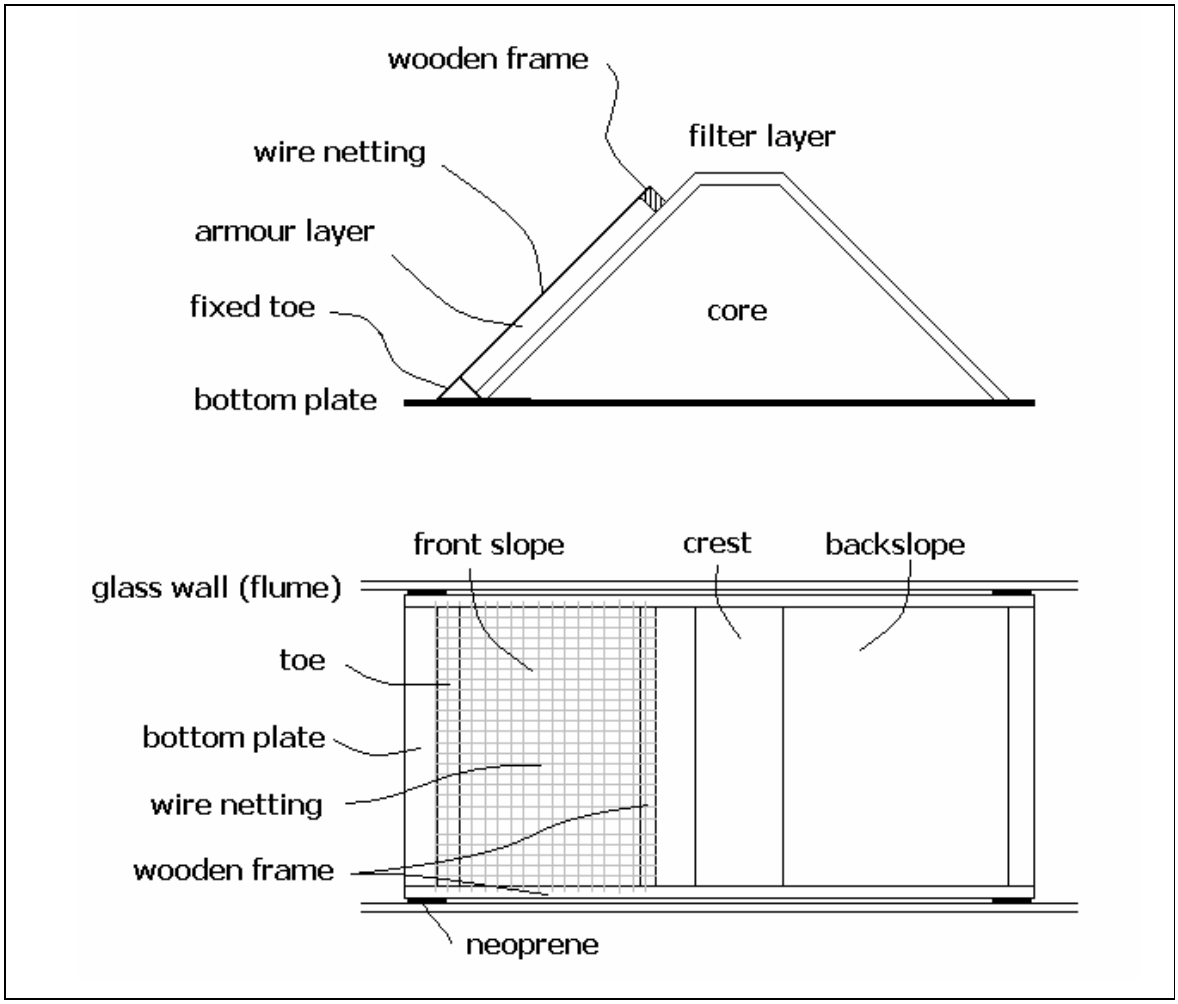

figure 3.6 Construction scheme of used breakwater, at the top: side-view, at the bottom : top-view

3.4.3 Test set-up

Wave conditions were measured by arrays of two gauges at "deep" water, halfway the foreshore and at the location of the structure toe. The analysis is based on the time series of the incident waves at the toe. These signals, without reflected waves, were obtained using the method by Goda and Suzuki (1976). This theory is developed for non breaking waves and valid in this experiment. Testing was performed initially with the structure in place and afterwards without the structure to check the accuracy of the software.

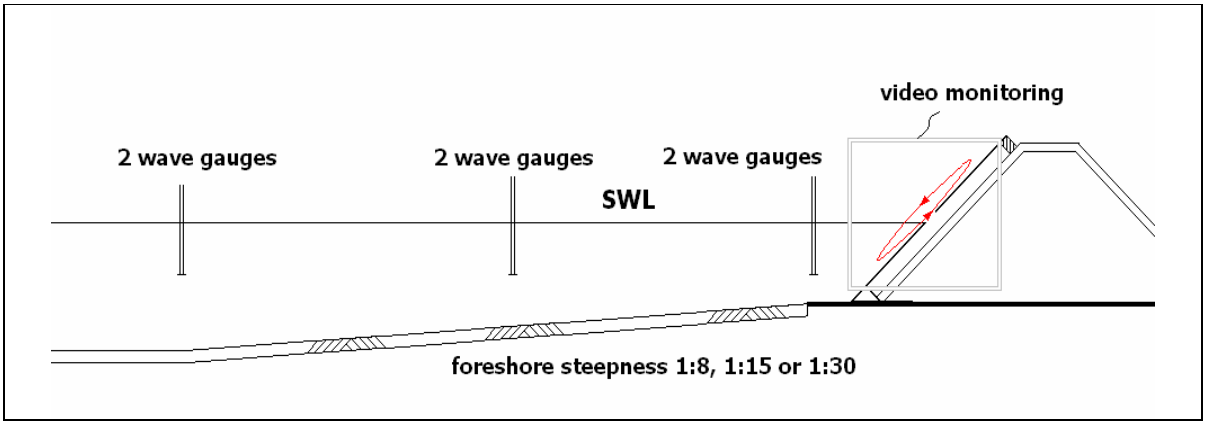

figure 3.7 Test setup

At the interface of the breakwater particles are being traced with a video camera. The location of the electro magnetic current meter is placed close to the toe at an elevation of 4cm from the bottom. This test setup is uniformly applied to all three different foreshores.

3.5 Test procedure

The following test procedure was used in advance of each test.

1. Calculate a suitable wave height and wave period.
2. Create the required still water level
3. Calibrate all six wave gauges
4. Use calculated wave height and period as input variables at wave board.
5. Measure wave height and wave period at the toe of the structure
6. Calculate incoming wave height and wave length at the toe of the structure
7. Repeat step 5. and 6. until the correct wave height and wavelength at the toe of the breakwater is obtained.
8. Start the wave board with the desired wave conditions at the toe
9. Record wave heights and velocity with wave gauges and EMS
10. Release zero buoyant particles at the breakwater interface
11. Record wave motion with video camera
12. Analyse wave record from wave gauges
13. Post process video film and convert images to displacements, velocity and acceleration data.
14. Conduct new experiment and repeat step 1. till 14 for all scenarios

The buoyancy of particles is a delicate item; therefore multiple tests are desirable to exclude inaccurate measurements.

3.6 Validity tests

To check the influence of different aspects of the experimental setup the following validity tests were taken:

1. Influence of the wire netting on wave reflection and run-up
2. Inertia of particles
3. Validity test of calculation of reflected wave height on a steep foreshore

3.6.1 Influence of wire netting

The influence of the wire netting on wave reflection was investigated in a conducted test. The breakwater was equipped with the wire netting. A pair of wave gauges placed at the toe measured the wave height. Series were conducted with a 3% steepness and wave heights of 6cm at the toe of the construction.

Afterwards the same wave conditions were used for the situation without wire netting. The wave height was measured and the reflected wave height was calculated. These tests were conducted three times, the averaged values are shown below.

Wave height 6cm, steepness 3% breakwater with wire netting

wave length	:	2.99 m
amplitude of incoming wave	:	0.03 m
amplitude of reflected wave	:	0.003 m

Wave height 6cm, steepness 3% breakwater without wire netting

wave length	:	2.99 m
amplitude of incoming wave	:	0.03 m
amplitude of reflected wave	:	0.003 m

From these tests it can be concluded that the difference in calculated incoming wave remains constant. So the influence of the wire netting can be considered justified in this experiment. Even in the calculated reflected wave height the value remained constant.

3.6.2 Software wave reflection on a steep foreshore

To calculate the reflection of a regular wave, a Matlab program Refreg has been written at the Laboratory of Fluid Mechanics, at Delft University of Technology. Goda and Suzuki have described the used method in 1976. In this method two wave gauges are used at a distance of about one fourth of the wavelength. This used method is based on linear wave theory. Since the experiment deals with a sloping foreshore and shallow water, the theory is not valid. To check whether the software calculated with an acceptable accuracy a test was set up.

Measurements were taken with a 1:8 foreshore with breakwater, and a 1:8 foreshore without breakwater. In the first case reflected waves from the breakwater were calculated at the location of the breakwater toe. Series were conducted with a 3% steepness and wave heights of 6, 8 and 10cm at the toe of the construction.

The same wave conditions were used for the situation without breakwater. The waves would not be obstructed by the breakwater and spilling breakers occurred at the 1:30 slope (since the 1:8 foreshore was built on the semi-permanent 1:30 foreshore). In this case at exactly the same

location (were the breakwater toe used to be) the wave height was measured and the incoming and reflected wave was calculated.

```
Wave height 6cm, steepness 3%
wave length                  :     2.017 m
amplitude of incoming wave   :     0.028 m
amplitude of reflected wave  :     0.004 m

Wave height 8cm, steepness 3%
wave length                  :     2.713 m
amplitude of incoming wave   :     0.041 m
amplitude of reflected wave  :     0.010 m

Wave height 10cm, steepness 3%
wave length                  :     3.340 m
amplitude of incoming wave   :     0.049 m
amplitude of reflected wave :     0.011 m
```

H_{toe} (with breakwater) [cm]	H_{toe} (no breakwater) [cm]	Deviation [%]
6,0	5,5	8,3
8,0	8,2	2,5
10,0	9,8	2,0

table 3.4 Calculated difference in wave height, with breakwater and without breakwater

In the experiment a deviation up to 8% was measured. This error is due to a software package which calculates the reflected wave height, and only takes into account the first harmonic of the reflected wave height. This deviation is rather high (maximum deviation of 8.3%), since the experiment was carried out in the right terms of use of the software package, e.g. the waves were not breaking at the structure.

3.7 Summary

The experimental test setup was described and the necessary equipment and facilities listed. Measurement of particle velocity and acceleration are done with a video camera. Wave heights are measured at the toe of the construction. Regular waves and bichromatic waves are used, with a steepness of 3, 4 and 6%. Used wave heights are 6,8,10 and 12cm. The still water level remains constant at 20cm depth at the toe of the breakwater.

In total, three different foreshores will be used. Due to practical aspects the 1:30 is the mildest foreshore and 1:8 the steepest. Also 1:15 foreshore steepness will be used.

Chapter 4 Interpretation of experimental data

This chapter treats the interpretation of the experimental data. The process of the post-data processing and the used programs are described. The experimental accuracy will be determined, and finally the obtained velocity and acceleration measurements will be analysed.

4.1 Description of data processing of the video images

The video data is processed in order to obtain the velocity and acceleration values of the experiments. The figure below shows an image of a video tape (figure 4.1). The camera focuses on the breakwater and records the wave motion at the breakwater interface.

By releasing zero buoyant particles at this interface and tracking these particles an impression of the particle displacement in time can be obtained. In order to get this result the video tape was divided into frames. This resulted in 25 images per second, as this was the sampling rate of the video recorder. By applying a sampling technique each individual picture could be separated into two different time frames. Therefore it was possible to get a higher sampling frequency of 50Hz, i.e. 50 images per second.

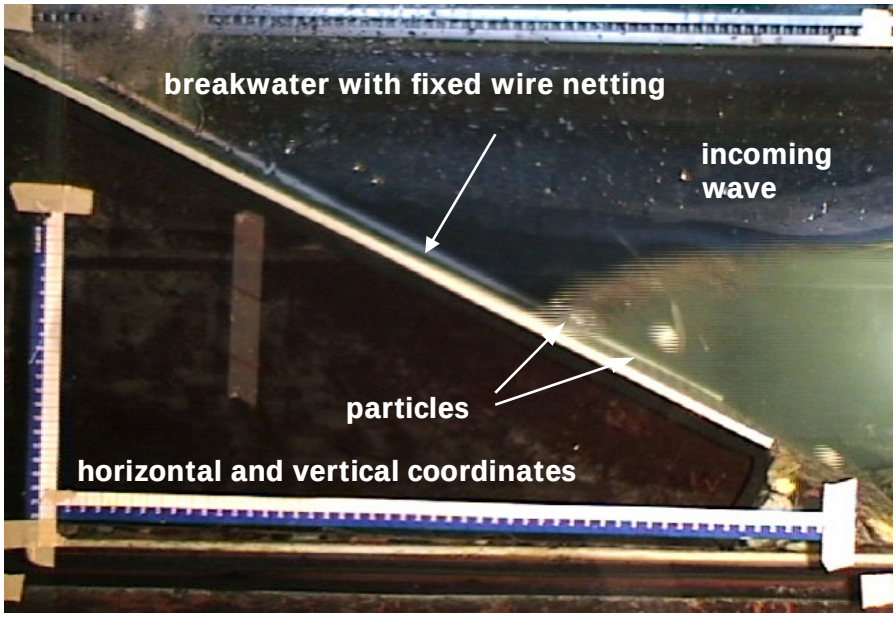

figure 4.1 frame from the video footage

Particle tracking was done with the software package MultiscanXY, which was supplied by the Fluid Mechanics Laboratory. Using this software it is possible to track manually the particle movement at a time step of 0.02 second. The position of the particle is recorded in a two dimensional pixel scale, see figure 4.2. The record of the particle displacement is written to a data file as a function of vertical position, horizontal position and moment in time.

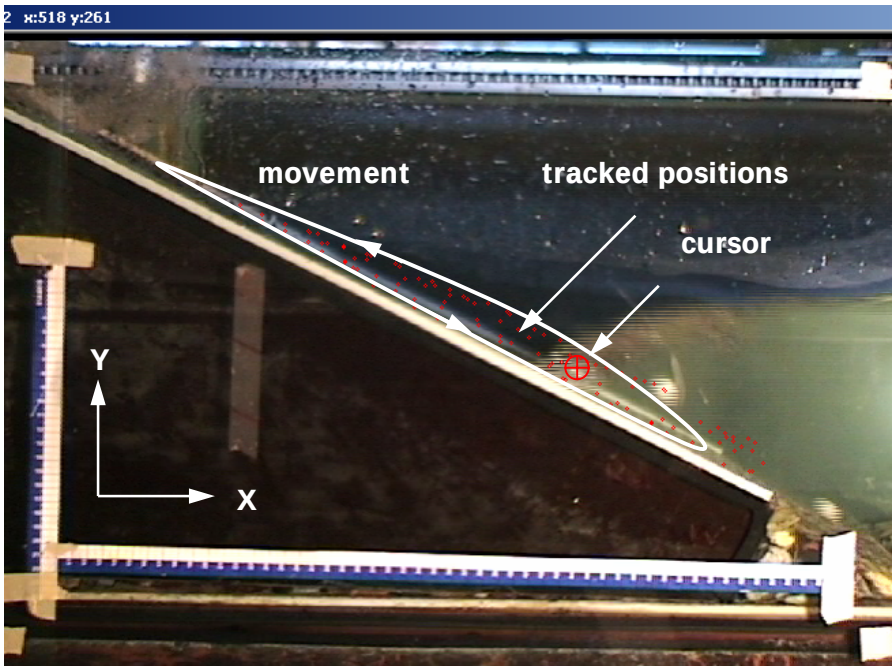

figure 4.2 tracking the particle (red dots) with MultiscanXY into pixel-coordinates.

By using a Matlab script called Vels, it is possible to transform the displacement unit from pixels into metric scale. First the axes are rotated into an exact vertical and horizontal alignment. The coordinates are marked on the flume and they represent an accurate vertical and horizontal reference system with respect to the water level and breakwater orientation. Due to a deviating camera angle it possible that the axes are rotated. As can be seen in figure 4.2 the picture is somewhat rotated (the chain rail is horizontal aligned). To account for this and to increase the accuracy of the experiment the transformation is necessary. For more information about the transformation process, see appendix B.

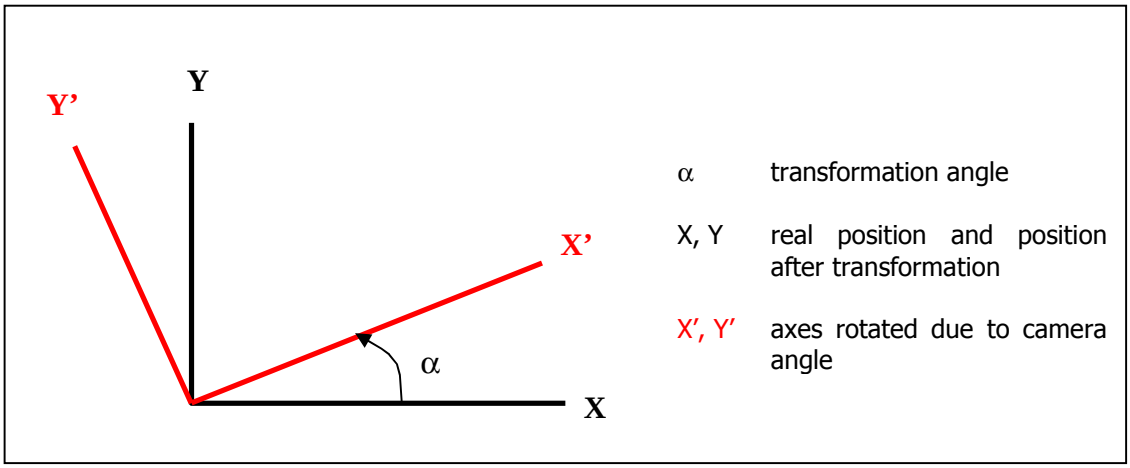

figure 4.3 Transformation process

With the accurate coordinate system it is possible to calculate the velocity and acceleration with respect to the breakwater slope. The velocity and acceleration are calculated parallel to the structures orientation and normal (tangent) to the breakwater orientation.

By differentiating the particle displacement in time, the velocity and acceleration in time is obtained. Results of a vector plot of the calculated velocity and acceleration are given in figure 4.4 and figure 4.5. The vector plots give a good indication of the fluid motion at the breakwater. The sizes of the vectors indicate the magnitude of the velocity or the acceleration. The starting point of the vector coincides with the position of the particle.

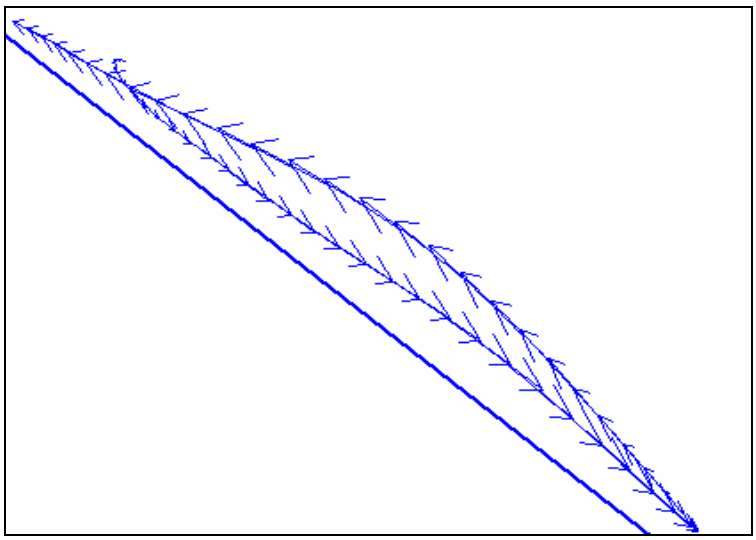

figure 4.4 vector plot of calculated velocity for one wave period, by Vels (Matlab script). The diagonal line indicates the position of the breakwater.

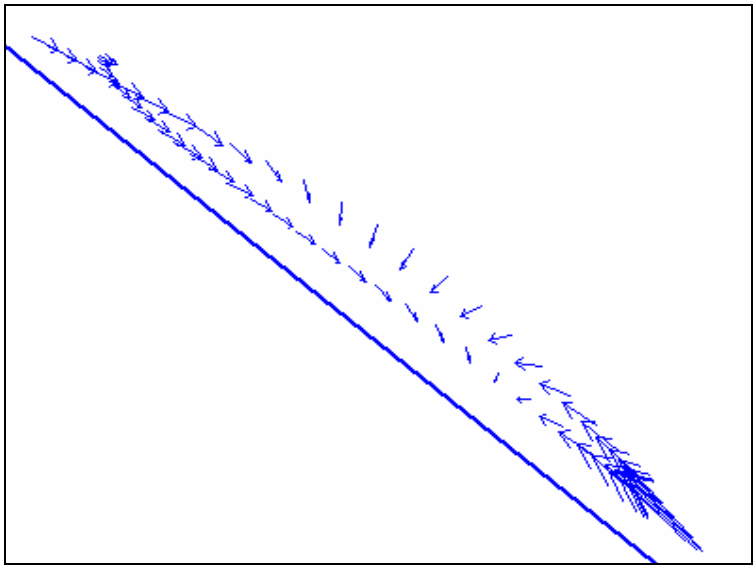

figure 4.5 vector plot of calculated acceleration by Vels (Matlab script). The diagonal line indicates the position of the breakwater.

The program Vels is also programmed to calculate the velocity and acceleration relative and tangent to the breakwater slope. These data are further used and processed to analyse the influence of the foreshore steepness on the fluid motion at the breakwater.

4.2 Measurement accuracy and reliability

In order to calculate the accuracy and reliability of the experiment, the type of distribution is necessary. It is assumed that the variables are normal distributed with a standard deviation equal to the absolute error and an expectation value given by the average low value, as defined in table 4.1.

table 4.1: Normal distributed measuring errors

Variable	Instrument	St.deviation	Mean value	Relative error
a) wave height	wave gauge	0.01cm	1cm	1.0%
b) wave period	wave gauge	0.01s	1s	1.0%
c) particle Inertia	Camera	1.0 cm	20cm	5.0%
d) incoming wave height	1st order wave refl.	0.5 cm	6 cm	8.3%
e particle tracing	Camera	1.0 cm	13.3 cm	7.5%
f) wave length	Lin. dispersion relation	1.0 cm	20cm	5.0%

The relative error of a function h(a,b) with measured variables a and b is calculated as follows:

$$r_h^2 = \left(\frac{\sigma_a}{\mu_a}\right)^2 + \left(\frac{\sigma_b}{\mu_b}\right)^2 \qquad (4.1)$$

Where:

σ	standard deviation of the measurement error	[-]
μ	mean value of the measurement error	[-]
r	relative error of the experiment	[-]

From this the relative error for the experiment is calculated. The relative error in the particle displacement measurement indicates 13%.

Another possibility to calculate the relative error for the experiment is given by the following set of equations:

$$r_h^2 = \left(\frac{\sigma_h}{\mu_h}\right)^2 \qquad (4.2)$$

$$\sigma_h^2 = \sigma_a^2\left(\frac{\partial h}{\partial a}\right)^2 + \sigma_b^2\left(\frac{\partial h}{\partial b}\right)^2 \qquad (4.3)$$

$$\mu_h = \frac{1}{n}\sum_{i=1}^{n} \mu_i \qquad (4.4)$$

Here the relative error is calculated from the standard deviation and mean value of all the variables. The mean value is simple to calculate, as it is the average of the mean value of all variables. The standard deviation is somewhat more difficult to compute. Since the total standard deviation is dependent on the individual influence of the error on the total outcome. However there is no function that describes the velocity or acceleration on a breakwater. One can make an estimation of it by regarding the differential as a weight function.

Variable	Instrument	$\partial h / \partial i$
a) wave height	wave gauge	1.10
b) wave period	wave gauge	1.10
c) particle Inertia	Camera	1.05
d) incoming wave height	1st order wave refl.	1.10
e particle tracing	Camera	1.05
f) wave length	Lin. dispersion relation	1.10

table 4.2 Estimations individual influence of the error on the accury

From this the relative error can be calculated and notes 19%. This is a relative error of the order of 5% higher than the other method. However, from both calculations it is clear that the relative error of the particle displacement is somewhere in the order of 13 to 19%. This large error in the output was more or less to be expected, since it was a complicated process, using different techniques to obtain the final results.

The velocity and acceleration is calculated, by differentiating the displacement in time. Using this method, the velocity value is calculated by using two displacement values. This decreases the reliability. The reliability for the velocity is thus, the square root of two times the reliability

Each measurement is repeated at least three times. This increases the measurement reliability with a factor $1/\sqrt{N}$, where N is the number of repeated experiments.

$$\frac{1}{\sqrt{3}}\sqrt{(13\sim 19)^2+(13\sim 19)^2}=\frac{1}{\sqrt{3}}\sqrt{2(13\sim 19)^2}\cong 10\sim 16\%$$

The same method applies for the calculation of the acceleration, where the reliability is;

$$\frac{1}{\sqrt{3}}\sqrt{(18\sim 27)^2+(18\sim 27)^2}=\frac{1}{\sqrt{3}}\sqrt{2(18\sim 27)^2}\cong 14\sim 20\%$$

4.3 Displacement analyses

The particle displacement is obtained by MultiscanXY. In the previous paragraph it was calculated that the relative error in the particle displacement is in the order of 10~16%.

The record of particle displacement is shown below. The record shows a regular incoming wave, surging on the breakwater slope. The displacement illustrates also a regular pattern; however it contains deviations in the minimum and maximum pattern. The minima and maxima show some fluctuations (peaks). These peaks are faults made during tracking of the particle. The error can

be caused by the visual disappearance of the particle, so a value had to be guessed, or perhaps the particle was not correctly tracked.

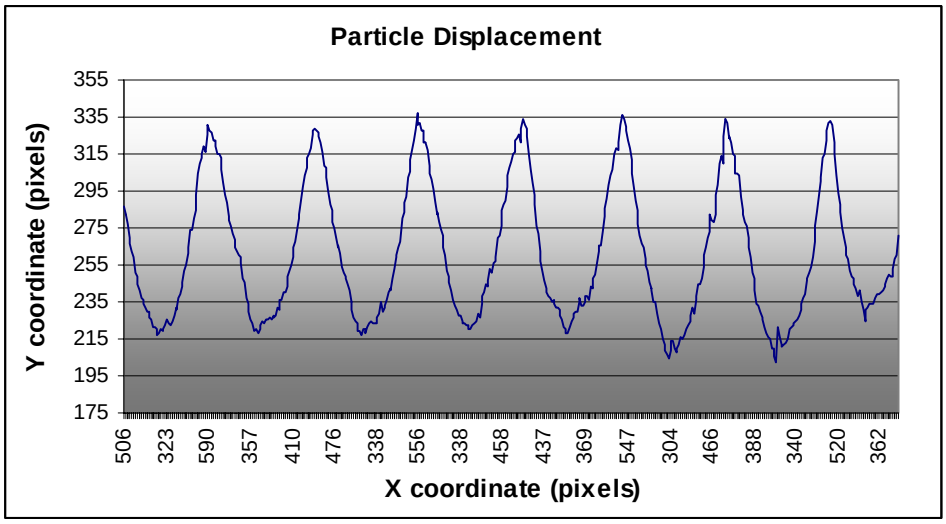

figure 4.6 particle displacement (by MultiscanXY) in pixel coordinates

Overall, the measuring method seems promising. The maxima and minima are rather constant, and also some kind of peakedness can be seen in the displacement pattern.

4.4 Velocity analyses

The velocity values are obtained by differentiating the particle displacement in time. A velocity registration is shown below. In the previous paragraph it was calculated that the relative error is in the order of 10~16%.

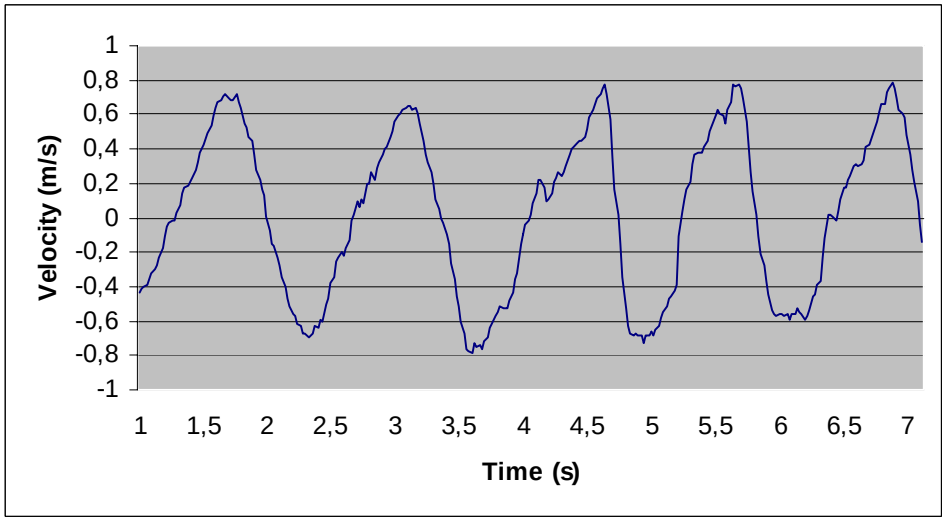

figure 4.7 velocity registration

The displacement shows some irregularities, this affects the velocity registration; as can be seen in figure 4.7. The maxima and minima show a certain error band. Also some secondary maxima and minima appear to be present. This is an artefact; it does not occur in the experiment, but exists due to the measuring technique and the data processing.

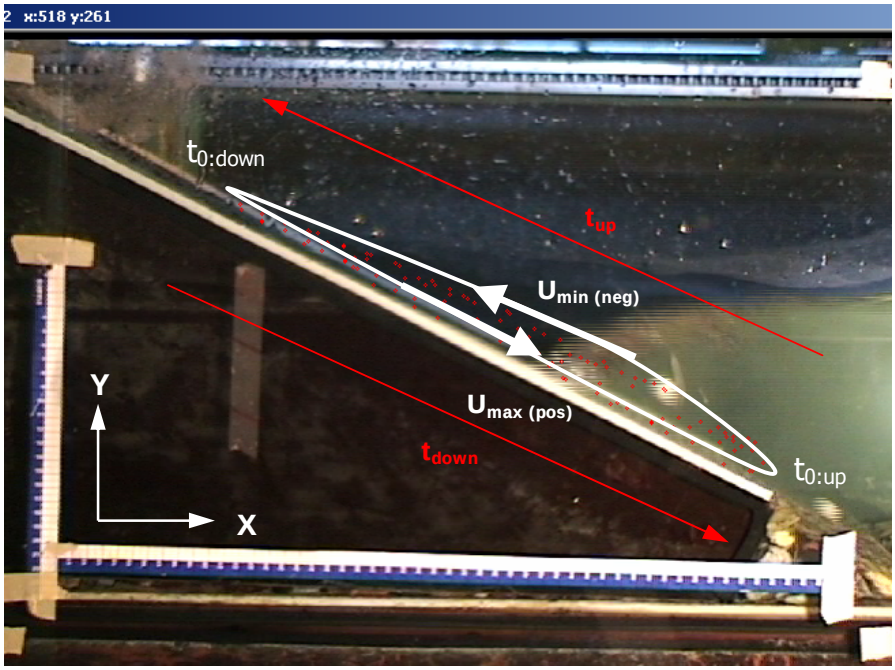

figure 4.8 Characteristic parameters

The downward movement is chosen as the positive direction. This results in a negative velocity value during up-rush and positive during down-rush, as illustrated in figure 4.8.

To analyse the velocity and be able to compare data with other measurements, specific parameters are chosen. The parameters are:

U_{max}	the local maximum velocity
U_{min}	the local minimum velocity
t_{max}	moment in time, which coincides with the maximum velocity
t_{min}	moment in time, which coincides with the minimum velocity
$t_{0:up}$	moment in time, where the velocity turns from a negative value to a positive value
$t_{0:down}$	moment in time, where the velocity turns from a positive value to a negative value

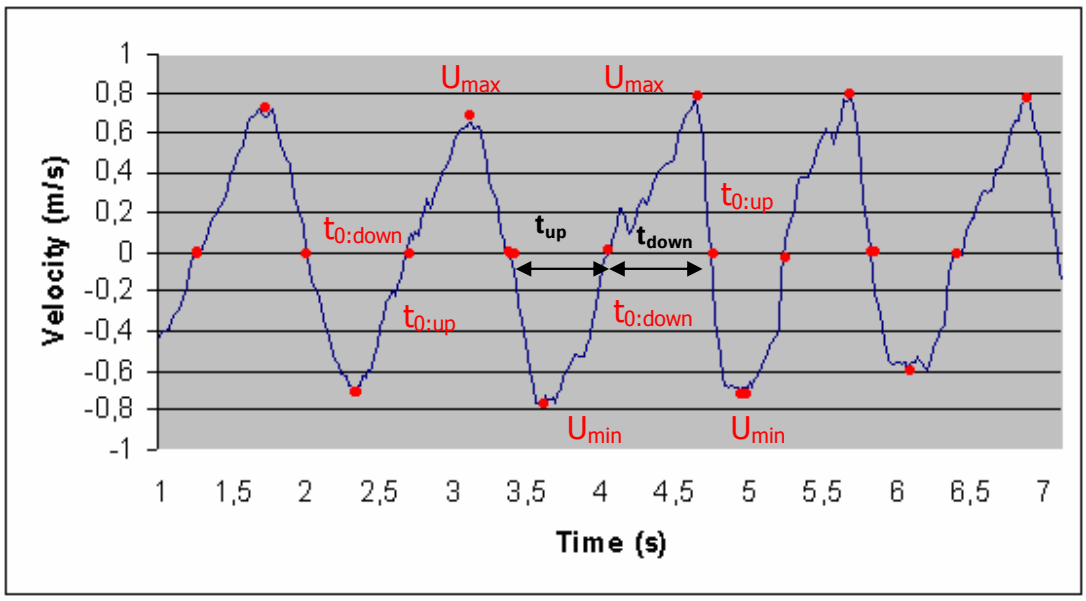

figure 4.9 velocity registration and chosen parameters

The velocity registration shows a clear spreading of the maxima. This spreading is due to all different measurement errors made during the experiment, tracking and calculation process.

The spreading of the maxima and minima is calculated by taking these values into account. By assuming a normal distribution of the error, the standard deviation and a mean maximum velocity can be calculated. The same routine is used, for the period of up-rush and down-rush.

The corrected graph with respect to measurement errors the graph would probably look like figure 4.10.

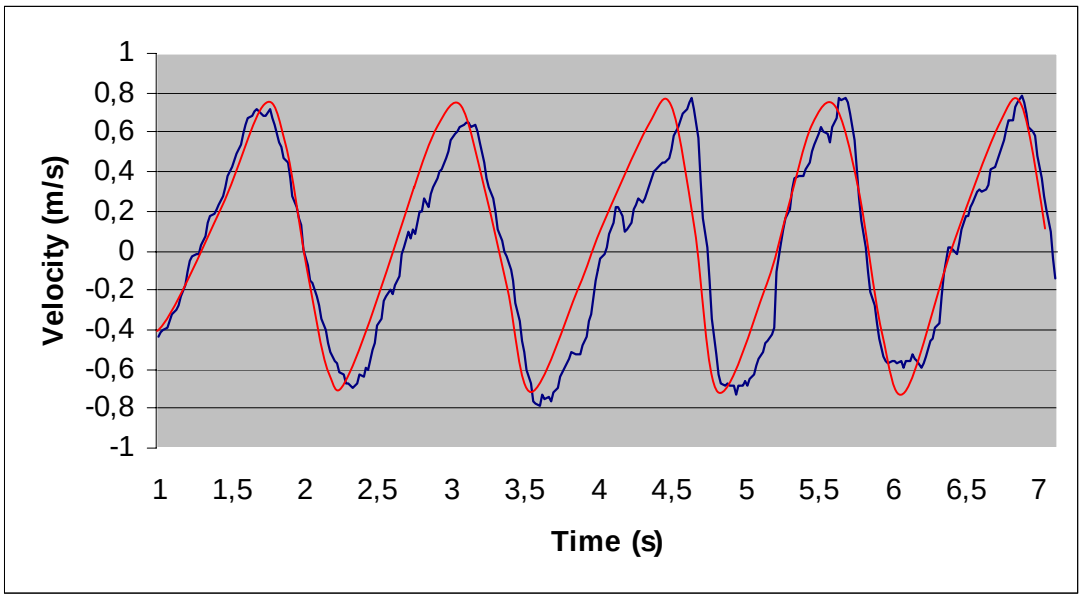

figure 4.10 Idealized velocity registration

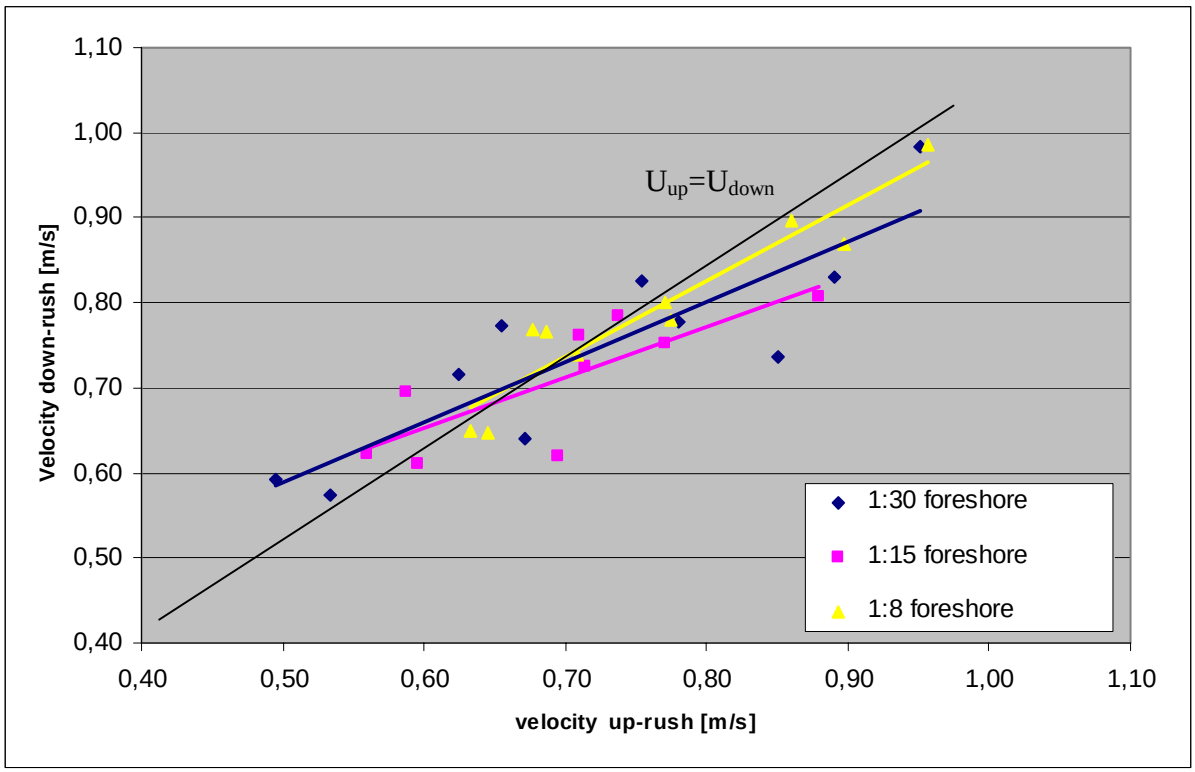

figure 4.11 Down-rush velocity versus up-rush velocity

In figure 4.11 the down-rush velocity is illustrated versus up-rush velocity. The velocity for down-rush is almost equal to the up-rush velocity. Also the obvious relation of increasing up-rush velocity and increasing down-rush velocity is shown in the graph. However in this representation no clear foreshore influence is illustrated.

In the next section the data is analysed and represented in such a way that influence of the foreshore steepness is illustrated.

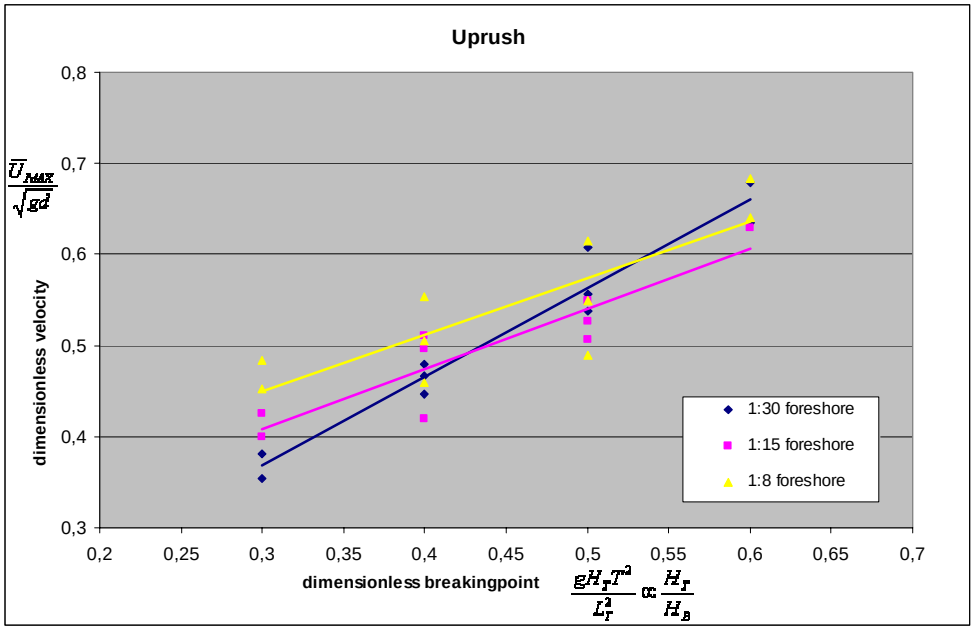

figure 4.12 Influence of the foreshore steepness on the dimensionless peak velocity at the breakwater for up-rush.

The notation in the graph represents:

$\overline{U}_{MAX}$	mean of the measured peak velocity at the breakwater slope for down-rush/up-rush	[m/s]
d	water depth at the toe	[m]
T	wave period	[s]
H_T	wave height at the toe of the breakwater	[m]
L_T	Wave length at the toe of the breakwater	[m]
H_B	Maximum wave height at the breaking point	[m]

The peak velocity, measured at the breakwater is made dimensionless with the square root over the gravitational acceleration and the water depth. In shallow water this represents the wave celerity. Since the particle velocity (represented by $\overline{U}_{MAX}$) in a progressive wave cannot exceed the wave celerity, otherwise wave breaking will occur. The vertical scale can thus be interpreted as a dimensionless breaking parameter. Since the water depth was kept constant, the wave celerity in shallow water is constant. The vertical axis can also be interpreted as the increase in the maximum velocity at the breakwater slope.

The horizontal axis represents the dimensionless ratio of the measured wave height at the toe and the breaker height defined by Miche in 1951. The background of this parameter is given in appendix D.

The above-described method is applied for both up-rush and down-rush, see figure 4.12 and figure 4.13.

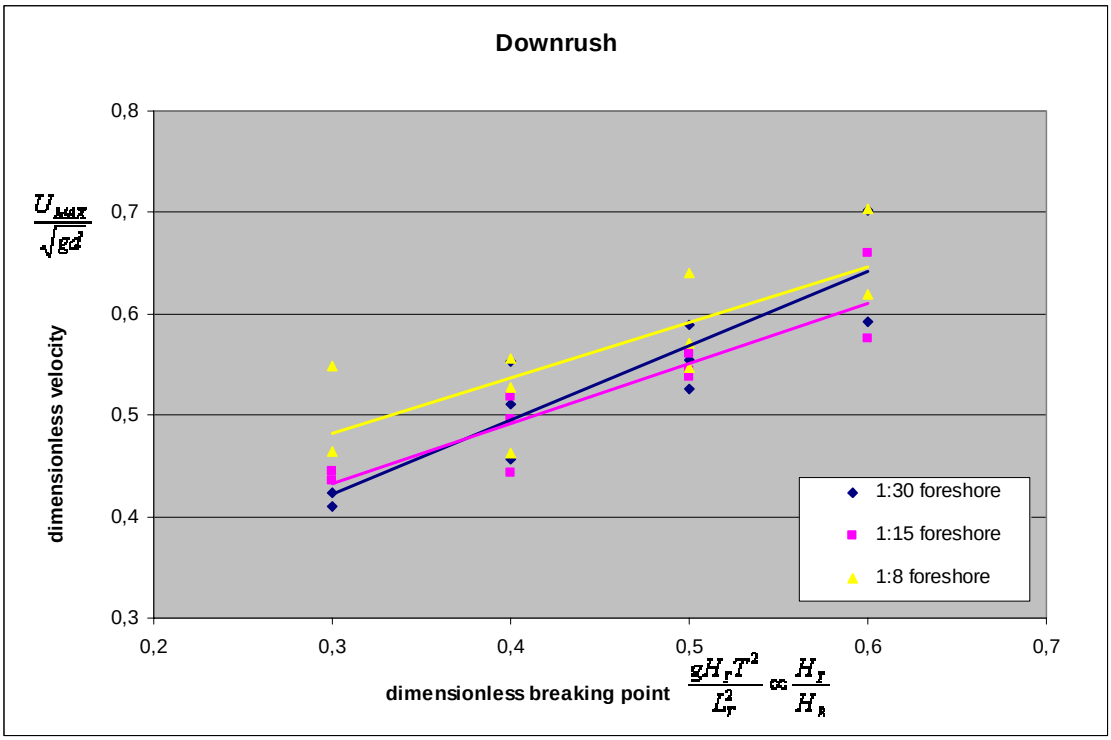

figure 4.13 Influence of the foreshore steepness on the dimensionless mean maximum velocity at the breakwater for down-rush.

For both up-rush and down-rush there is a difference in the measured velocity at the breakwater for variable foreshore steepness.

For a small ratio of H_T/H_B the difference in the velocity at the breakwater is relative large for a variable foreshore steepness. For both up-rush and down-rush the largest velocity values are obtained for the steep 1:8 foreshore. The velocities for the 1:15 and 1:30 are lower. Interesting to see is that for both figures the differences between the 1:15 and 1:30 foreshore are relative small.

For an increase in the ratio of H_T/H_B the velocities increase for all foreshore steepnesses.

As the ratio of H_T/H_B reaches the value 1, i.e. wave breaking, the differences in velocity values for the variable foreshore steepnesses reduce. This can imply that the difference in velocity reduces, as the point of wave breaking is reached. When the particle velocity reaches the speed of the wave propagation speed, the wave becomes instable and will break. For up-rush the reliability decreases for velocity values near the breaking point. This increase in scatter coincides with the experience that the used experimental method was not suited in case of wave breaking. Tests with the highest and steepest waves (wave height 12cm and steepness 6%) showed during the experiment to be close to wave breaking. By calculation of the breaker parameter (Iribarren) ξ=2.6. This indicated that indeed the breaker type is close the collapsing type, instead of a surging breaker.

By extrapolating the fitted trend line, the relation between the breaking criterion of Miche and wave breaking due to exceedance of the wave celerity by the particle velocity is shown, see figure 4.14. Both relations imply that for the dimensionless value of the breaking point for a value

of 1, wave breaking should occur. Both breaking criterions meet in the order of 1, as would be in the expectation of theory. The deviation for a 1:8 foreshore steepness is somewhat larger (H_T/H_B ≅1 and $\overline{U}_{MAX} / \sqrt{gd}$ ≅0.85).

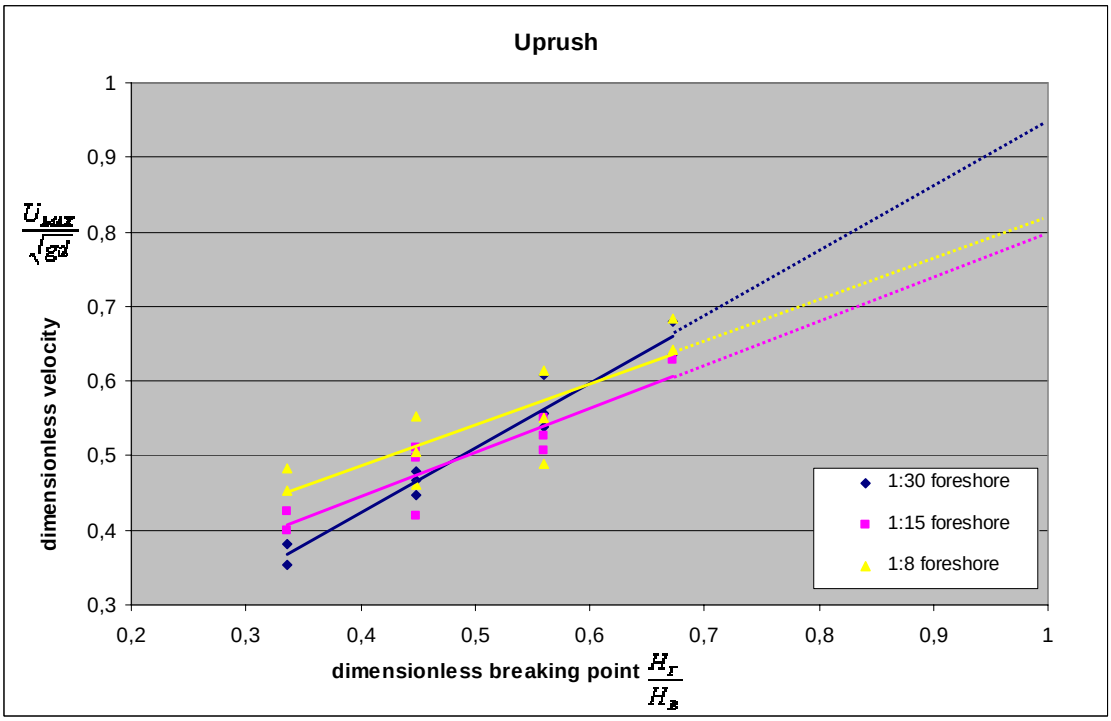

figure 4.14 Extrapolation of experimental data, influence of dimensionless

As mentioned before, the velocity data converges near the point of wave breaking. The point of wave breaking is defined by Battjes in 1974 for a surf similarity parameter of 2.3. In figure 4.15 the measured velocities are represented by their breaker parameter, i.e. surf similarity parameter. The figure shows that close to wave breaking the measured velocities are nearly similar per foreshore steepness. For larger values of the breaker parameter the breaker type is collapsing and surging.

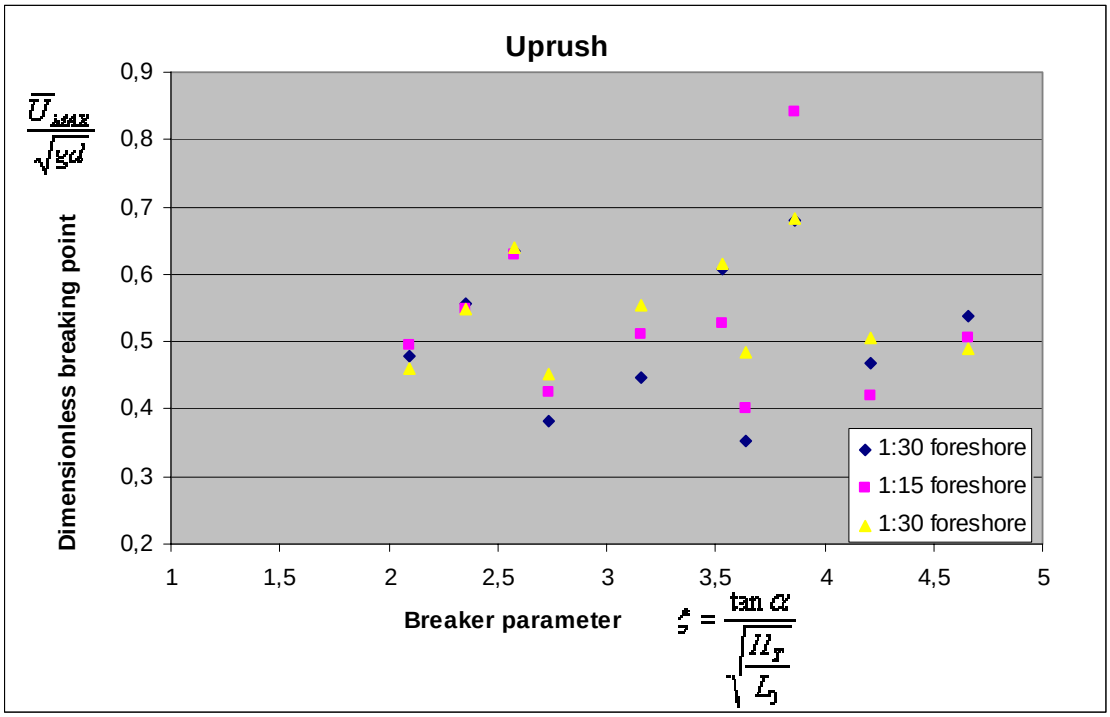

figure 4.15 measured mean maximum velocity represented by the breaker parameter and foreshore steepness.

In figure 4.16 and figure 4.17 the peak velocities of the relative steep foreshores (1:8 and 1: 15) are plotted versus the mild foreshore (1:30). This method is used for both up-rush (figure 4.16) and down-rush figure 4.16.

The figures show that the velocities for the steepest foreshore are slightly higher than for the milder slopes. This relation exists for both up-rush and down-rush. For higher velocities the difference for variable foreshore steepness reduces. Increase in velocity coincides with an increase in wave height and wave steepness.

The figures also illustrate that for increasing wave height and steepness (increasing velocity) the 1:30 data shows a different trend than the steeper foreshores. This trend seems strange, since the 1:8 and 1:15 velocity trend behaves more or less the same, except that higher velocities are measured for the steep foreshore. This "behaviour" occurs for both up-rush and down-rush.

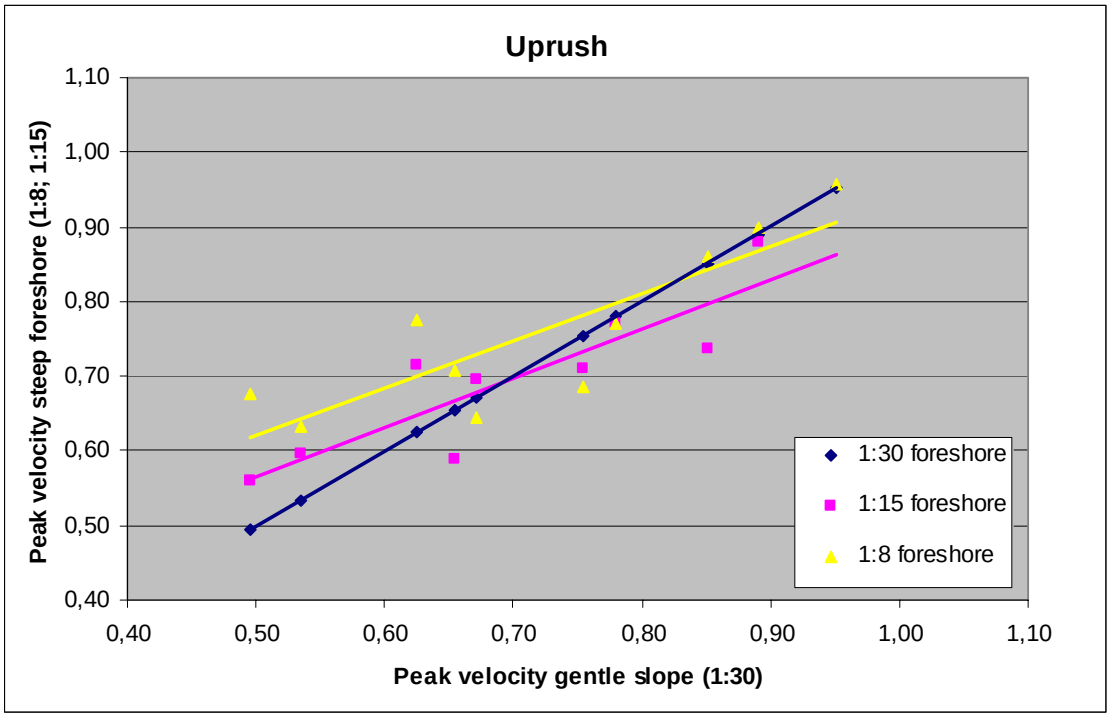

figure 4.16 Peak velocity steep foreshores (1:8 and 1:15) as a function of the gentle foreshore (1:30). for up-rush.

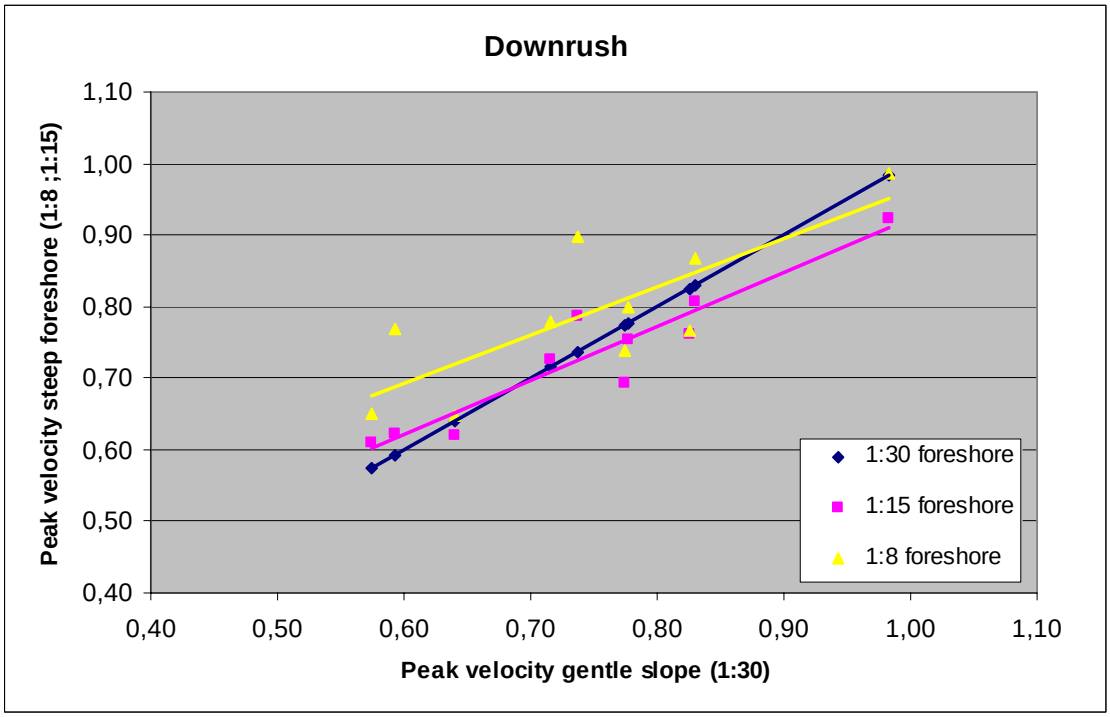

figure 4.17 Peak velocity steep foreshores (1:8 and 1:15) as a function of the gentle foreshore (1:30). for down-rush.

Considering the relative error of 10% in the velocity values, visualised in figure 4.18, the error band covers all measurements. This means that the differences in the measurements for variable foreshore steepness lie in the range of the error margin. Therefore no valid conclusions could be drawn. However the measurements show a clear trend, indicating that the measurements do not consist of random errors on a large scale. Also the relative error is calculated on the highest errors of the lowest measured values, i.e. the relative error is calculated on the high side.

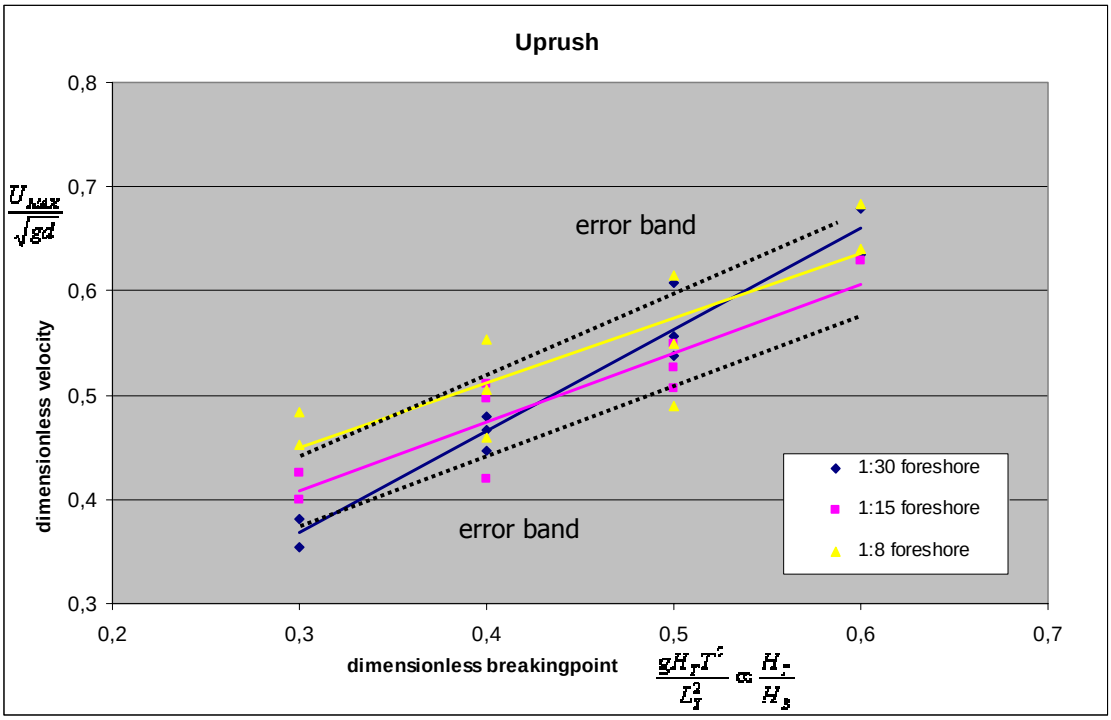

figure 4.18 Dimensionless mean maximum velocity for different foreshore steepnesses and a errorband of 10%. The error band is drawn around the data of the 1:15 foreshore.

4.5 Acceleration analyses

The acceleration values are obtained by differentiating the particle displacement in time. A velocity registration is shown below. The calculated relative error is in the order of 14~20%. Since the data of the acceleration is very irregular the data is smoothened by using a 7-points moving average. In figure 4.19 an acceleration profile is illustrated. The figure becomes rather irregular and shows secondary peaks.

The analyses of the acceleration data follow the same procedure as the velocity data. The chosen parameters are:

A_{max} the local maximum acceleration
A_{min} the local maximum velocity
t_{max} moment in time, which coincides with the maximum acceleration
t_{min} moment in time, which coincides with the minimum acceleration
$t_{0:up}$ moment in time, where the acceleration turns from a negative value to a positive value
$t_{0:down}$ moment in time, where the acceleration turns from a positive value to a negative value

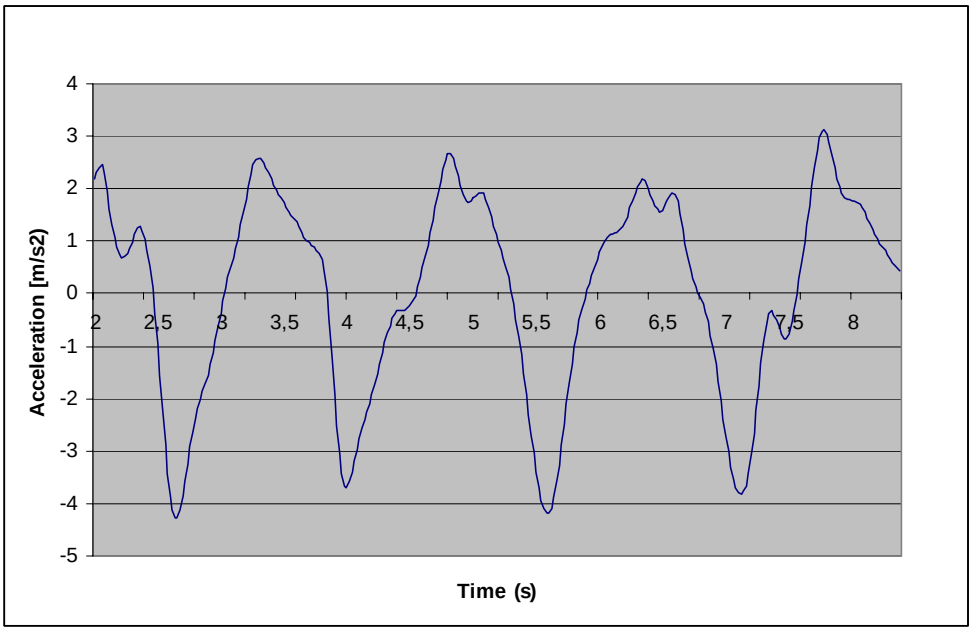

figure 4.19 Acceleration profile with a 7-point moving average.

For both up-rush and down-rush there is a difference in the obtained acceleration at the breakwater for variable foreshore steepness.

As the ratio of H_T/H_B increases, i.e. the wave becomes closer to the point of wave breaking, the acceleration values increase.

For both up-rush and down-rush the highest accelerations are derived for the steepest foreshore. The largest accelerations are measured during up-rush. The scatter in the data is relative large.

Differences in value for peak accelerations during up-rush and down-rush are roughly a factor two. The highest accelerations are measured during up-rush. Lower accelerations are obtained during down-rush. The lower values are obtained, since during down-rush the water flows down the breakwater. During up-rush the fluid is accelerated by the momentum of the wave.

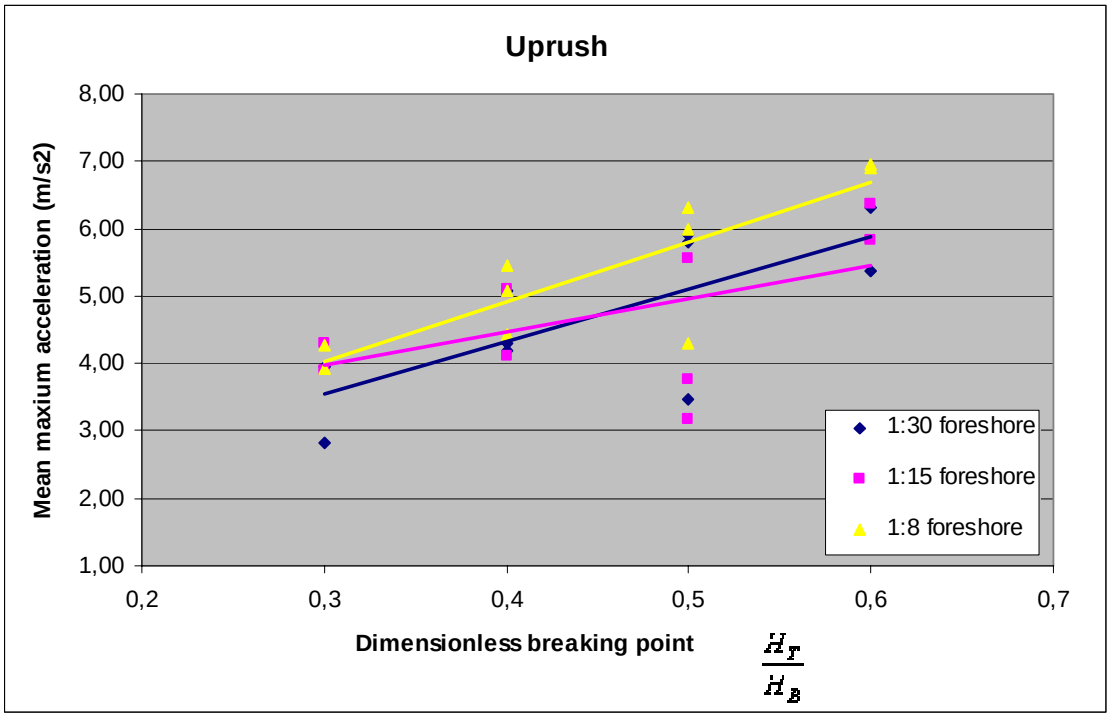

figure 4.20 Influence of the foreshore steepness on the mean maximum acceleration at the breakwater for up-rush.

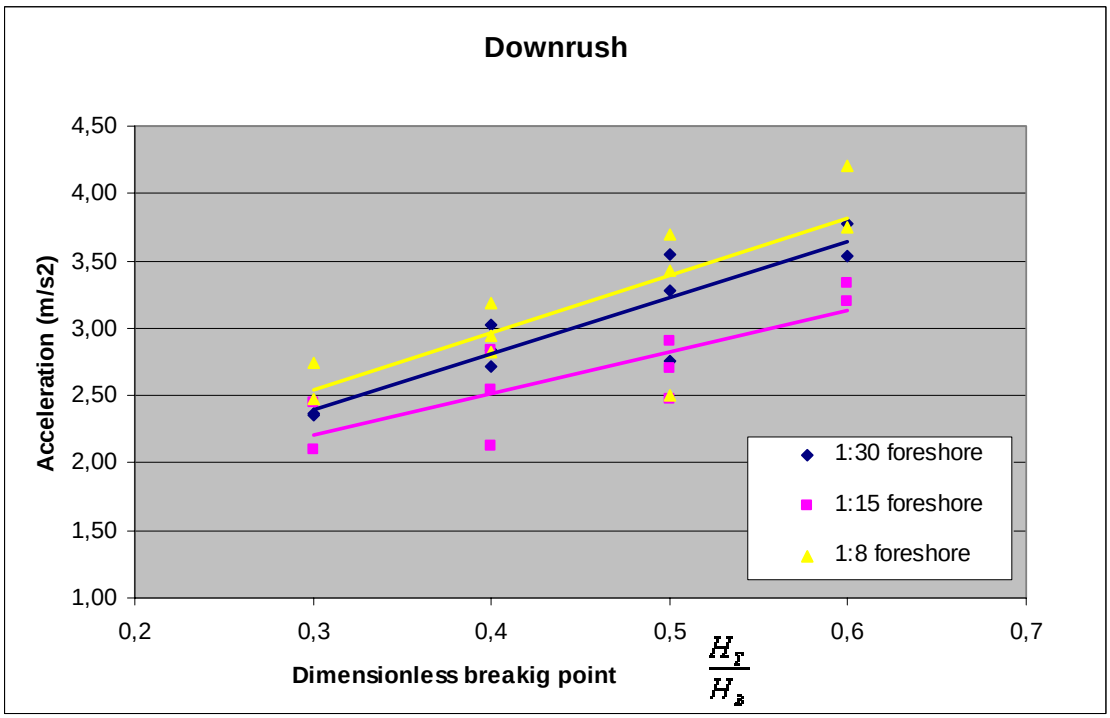

figure 4.21 Influence of the foreshore steepness on the mean maximum acceleration at the breakwater for down-rush.

In figure 4.22 and figure 4.23 the peak accelerations of the relative steep foreshores (1:8 and 1:15) as a function of the peak acceleration at the relative gentle foreshore steepness (1:30).

The largest accelerations for both up-rush and down-rush are obtained for waves travelling over the steep foreshore. For up-rush the peak accelerations lie in a close range, the smallest peak accelerations are observed for the mildest foreshore steepness. However, for down-rush the smallest peak accelerations occur for the 1:15 foreshore steepness and not for the 1:30 slope.

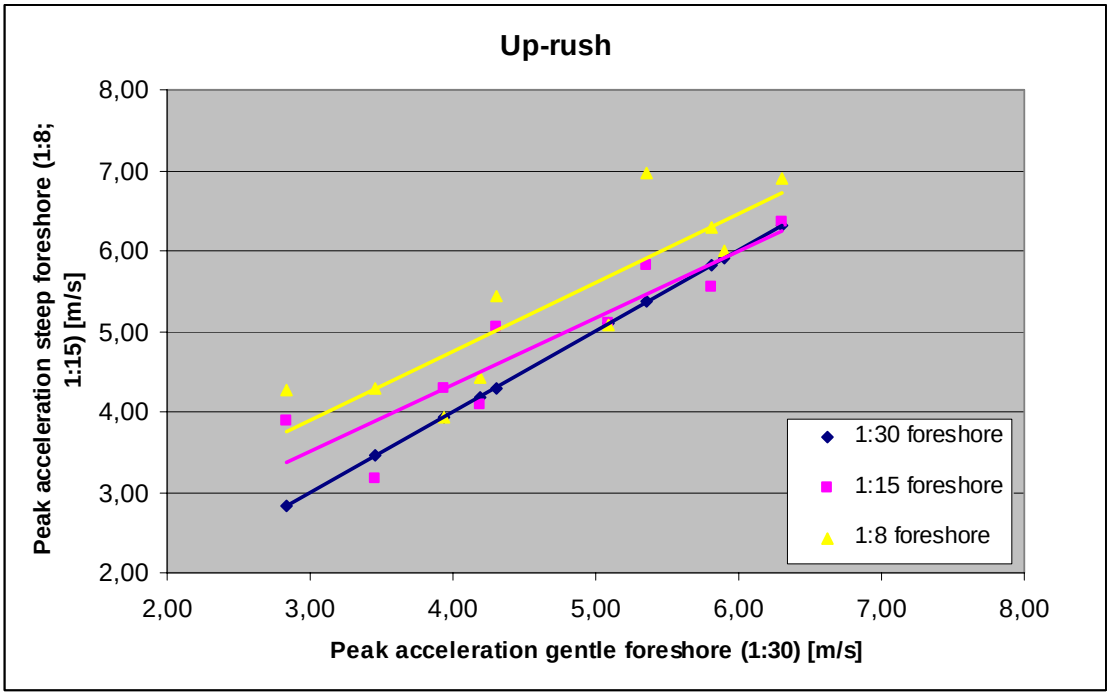

figure 4.22 Peak acceleration of the relative steep foreshores (1:8 and 1:15) as a function of the relative gentle foreshore steepness (1:30) for up-rush.

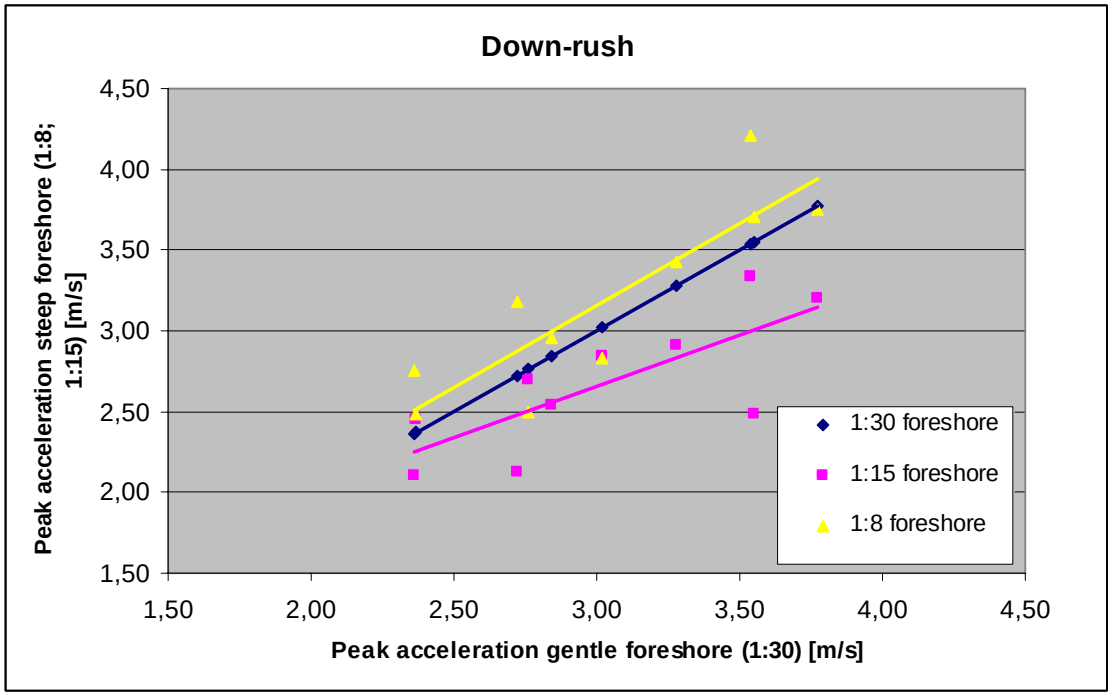

figure 4.23 Peak acceleration of the relative steep foreshores (1:8 and 1:15) as a function of the relative gentle foreshore steepness (1:30) for down-rush.

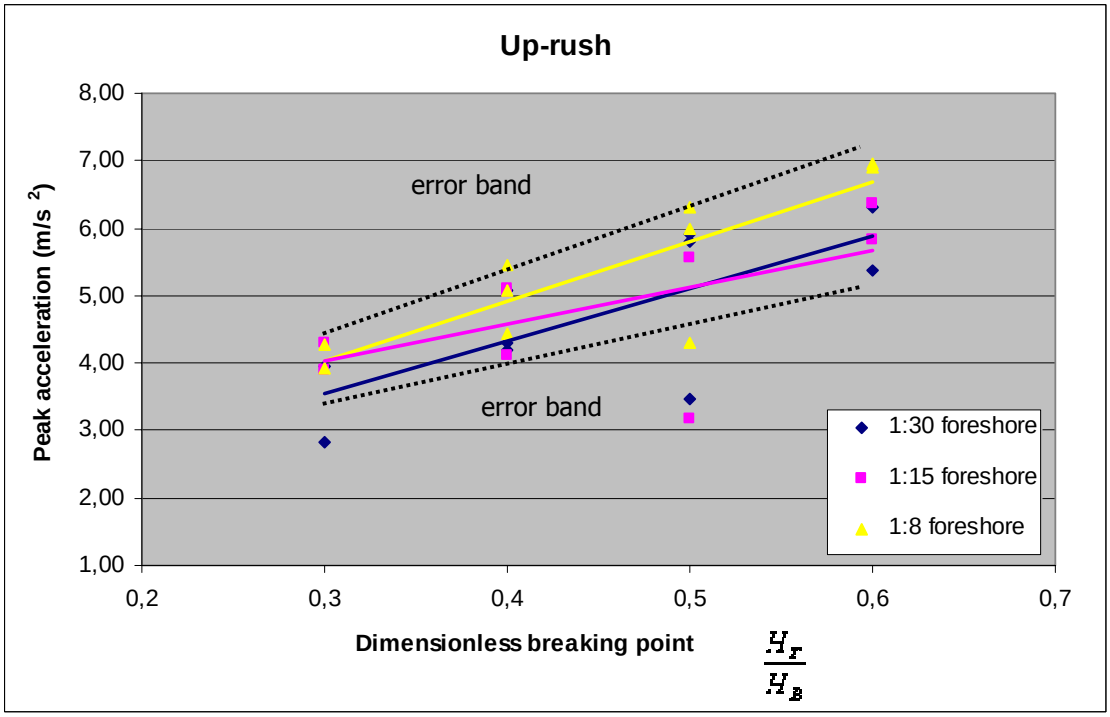

figure 4.24 Mean maximum acceleration for different foreshore steepnesses and an errorband of 14%.

When considering the error band (estimated for the acceleration data in the range of 25%) the data for variable foreshore steepness lie in this range. This is illustrated in figure 4.24. The difference in acceleration per foreshore steepness lies in the error band.

4.6 Wave Analyses

Wave heights were measured near the wave board, halfway the foreshore and at the toe of the breakwater. The wave height and wavelength were kept constant at the toe of the breakwater per test for variable foreshore steepness. At the wave board regular waves were created. The development of a sinusoidal wave to a nonlinear wave, due to shoaling is shown in figure 4.25.

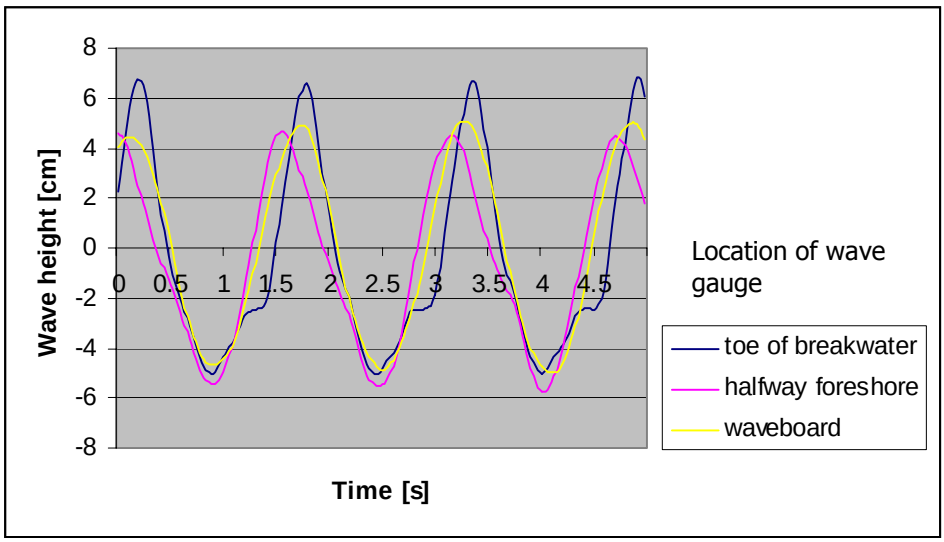

figure 4.25 Wave signal form wave gauges at a 1:15 foreshore steepness. The wave height is measured close to the wave board, halfway the foreshore and at the toe of the breakwater.

From the velocity and acceleration data is become obvious that there are differences is measured acceleration and velocity for waves travelling over a different bed slope. It seems logical that there should be differences in the wave signal.

However it is difficult to sign any differences in the wave signal due to the difference in foreshore steepness. First it must be mentioned that it is tried to vary only the foreshore slope steepness, however this includes some complications.

The water depth at the wave board is kept constant and so is the water depth at the toe of the structure. But when the steepness is varied, the waves are travelling not over only a changing bed slope. For an steep slope, the waves are travelling over a relative short section of foreshore. For a gentle slope the waves are travelling over a relative long foreshore (see figure 3.2). It seems logical that the length of the foreshore can play a role too.

In figure 4.26 a wave signal is given with a constant wave height (based on the incoming wave height) and steepness for the three different foreshore steepnesses.

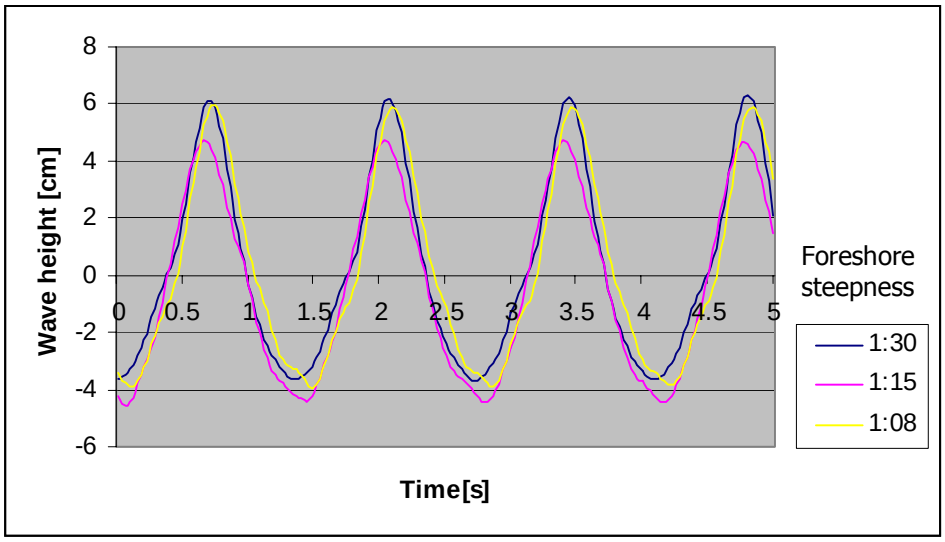

figure 4.26 Constant wave height and wave length for variable foreshore steepness. The wave signal is not separated, e.g. the reflected wave is included in the signal.

Drake and Cataloni suggested a parameter, which describes the peakedness of a dataset. This can be applied for the momentaneous amplitude of the wave signal, the velocity signal or the acceleration. For the amplitude of the wave the formula is:

$$a_{spike} = \frac{\overline{a^3}}{\overline{a^2}} \qquad (4.5)$$

a	the momentaneous amplitude	[m]
a_{spike}	parameter which describes the peakedness of the dataset	[m]

The range of the parameter a_{spike} varies with a factor ten. The fluctuation of this parameter varies in a range with is equal to repeating the same experiment (for increasing accuracy) and data for different foreshore steepnesses. No conclusions about wave peakedness can be drawn based on this parameter.

The parameter was also used for the velocity data. Also the use of this parameter did not contribute to classifying differences in the peakedness of the velocity signal. Since the acceleration is a function of the velocity

4.7 Foreshore steepness and stability

Since no actual damage tests are performed it is not possible to come up with a relation to damage and the difference in foreshore steepness. However, when it is assumed that the wave force shows a direct relation to the damage of the breakwater construction (failing armour layer) a foreshore steepness relation can be developed.

From the theory it is known that the wave force is equal to:

$$F_{wave} = \frac{1}{2} C_B \rho A u|u| + C_M \rho V \frac{Du}{Dt} \qquad (4.6)$$

Thus it can be made up that the wave force is equivalent to the velocity squared and linear with the acceleration term:

$$F_{wave} \propto c_1 \cdot u^2 + c_2 \cdot a \qquad (4.7)$$

u instantaneous velocity
a instantaneous acceleration
c_1 constant
c_2 constant

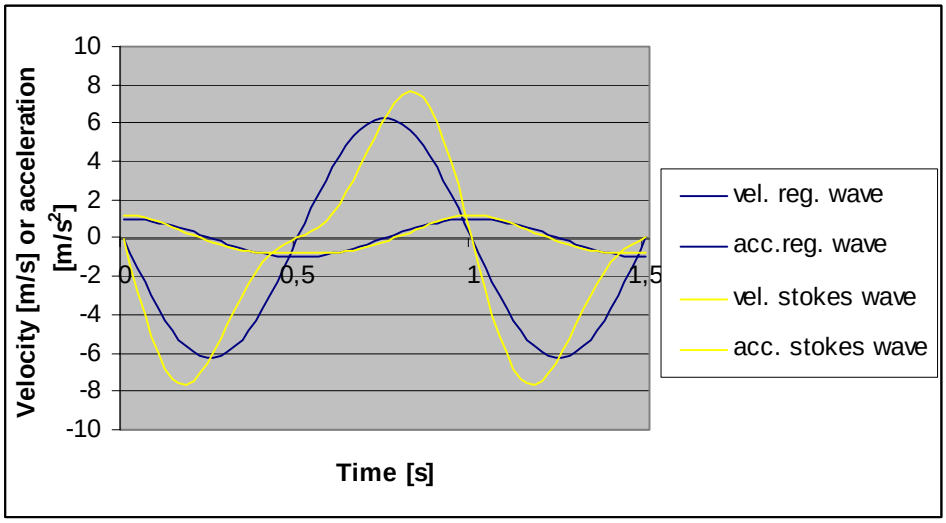

figure 4.27 calculated velocity and acceleration for a regular wave and a Stokes wave.

The figure above shows the difference in phase shift between velocity and acceleration, and the relative increase in acceleration for a regular and a Stokes wave. The velocity is in the same order, but the phase shift and the magnitude of the acceleration is different due to the nonlinearity of the wave.

When using the same coefficients for C_B and C_M as Tromp (2004) the wave force can now be computed, considering the surface area (A) as the diameter squared and the volume (V) as the diameter of the used rock to the power three.

Due to the phase shift and the relative increase in acceleration the wave force is for the Stokes wave in the order of 35% higher.

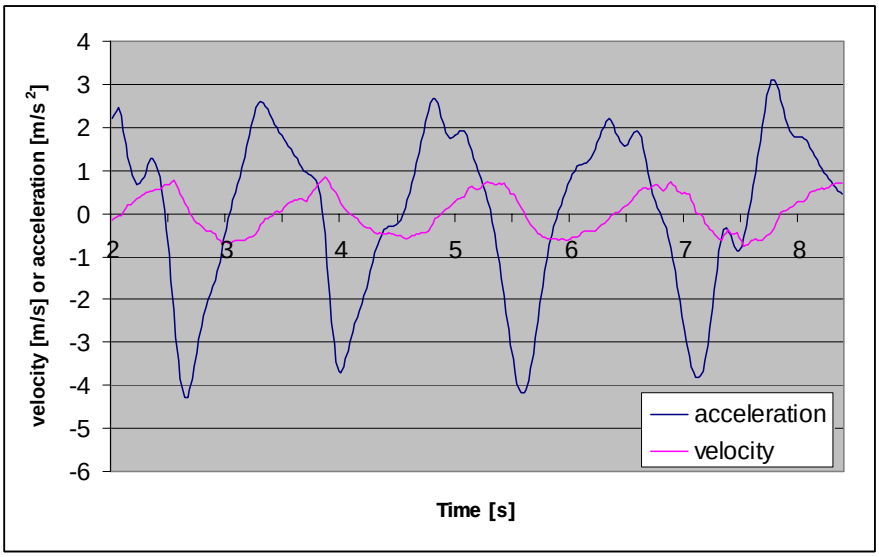

figure 4.28 velocity and acceleration registration, negative values illustrate up-rush, positive values coincide with down-rush

In figure 4.28 velocity and acceleration registration from the experiments is shown. The figures shows that due to the non linearity of the wave, the velocity and acceleration profile becomes more peaked and also a phase shift occurs between the velocity and acceleration profile.

For a momentaneous maximum velocity the acceleration still has a zero value. However close to the maximum velocity the acceleration already has a value in the order of -3 m/s^2. This is one of the aspects Tromp [2004] concluded and that a Morrison approach seems appropriate.

The velocity data (paragraph 4.4) shows a maximum difference of 10% for the relative steepest slope compared to the mildest foreshore. Considering only the increase in velocity terms and neglecting the acceleration term, the difference in wave force is 20% higher on a steep foreshore than on the gentle slope. Keeping in mind that the acceleration term shows also some increase for a steeper foreshore the wave force can even be higher than the given percentage (when assuming that the phase shift is in the same order).

For equal wave spectra at the toe of a coastal structure significantly more damage (order of 30%) occurs to a steep foreshore in contrast to a mild slope, Hovestad [2005]. By following the above theory and coupling the velocity and the acceleration to the wave force, the difference in damage can be explained for an equal wave spectral energy density spectrum for wave travelling over variable foreshore steepness.

4.7 Evaluation

For the experimental data a clear difference in velocity at the breakwater slope exists for variable foreshore steepness. Largest values occur in the experimental data for the steep 1:8 foreshore and the relative milder 1:15 and 1:30 slopes. The difference in velocity for equal wave conditions at the toe, between a 1:15 and a 1:30 foreshore is relative small. Velocities for up-rush are in the same range as for down-rush.

For an extrapolation of the data series, the breaker criterion of Miche and the breaking criterion of exceedance of the particle velocity over wave speed are shown. For up-rush the extrapolated

data crosses the breaking criterion in the order of one, which suggests wave breaking with both criteria. The experimental data fits this theory very well.

Differences in acceleration at the breakwater slope are obtained for variable foreshore steepnesses. The largest accelerations occur for the steep foreshore. The milder slopes register lower values of accelerations. Acceleration values for up-rush are in the order of twice as high as acceleration for down-rush.

In all cases the largest values for velocity and acceleration measurements for both up-rush and down-rush are obtained for the steepest foreshore. The other measurements show that the mildest foreshore shows the lowest velocity and acceleration values. The 1:15 foreshore lies between these values. This overall picture applies to almost all measurements. Only the acceleration for the 1:30 foreshore for down-rush is higher than for the 1:15 foreshore.

For the velocity measurements the 1:30 foreshore trend shows higher velocities for extrapolated increasing wave height and wave steepness. The linear fit is the best computed fit. This excludes the idea that another trend is more appropriate. However, this trend seems odd.

By applying the Morrison equation for calculating the wave force as a function of wave velocity and acceleration the wave force for waves travelling over a steep foreshore can be up to 20% higher than for waves travelling over a gentle foreshore. Since the relation between the coefficients is not known, the acceleration term is not calculated. The acceleration term has a linear relation to the wave force. Since the acceleration values are also higher for waves travelling over a steeper foreshore, this term adds up to the force exerted by the velocity term.

Hovestad [2005] concluded that for equal wave spectra at the toe of a coastal structure significantly more damage (order of 30%) occurs to a steep foreshore in contrast to a mild slope. Using the Morrison equation on the experimental data this difference can be explained due to the difference in velocity and acceleration for equal wave height and wave length at the toe of the structure.

Chapter 5 Conclusions and recommendations

This Master's Thesis was a pilot research project in order to investigate which parameters, other than the wave energy density spectrum, could play a role in breakwater damage on variable foreshore steepness.

The research project showed a qualitative difference in velocity and acceleration registrations at the breakwater interface for waves travelling over different foreshores.

5.1 Conclusions

- For both up-rush and down-rush consequently the highest peak velocities were registered for the steepest foreshore. Differences in peak velocity can range up to 15% due to difference in foreshore steepness.
- For both up-rush and down-rush consequently the highest peak accelerations were registered for the steepest foreshore.
- However, regarding the reliability analyses the range of differences in velocity and acceleration measurements lies in the error band. This could imply that the measured velocities and accelerations coincide with measurement errors. The velocities and accelerations per foreshore show a trend and the irregularity of this trend is relative small.
- Velocities for up-rush and down-rush are almost identical. Down-rush shows a slightly higher velocity pattern
- Accelerations are for down-rush significantly lower than for up-rush; in the range of a factor two.
- The peakedness of the wave-amplitude, velocity or acceleration cannot be described by the peakedness parameter of Drake and Cataloni for this dataset.
- Using the Morrison equation for calculating the wave force an increase in wave force is obtained for waves travelling over a steep foreshore, compared to waves travelling over a gentle foreshore. The increase in wave force due to the increase in velocity measured at the breakwater interface is up to 20%. The acceleration term also contributes to the increase in wave force. The relation however is not exactly known.
- The results of Hovestad [2005] coincide with the data and conclusions of this Master's Thesis. Hovestad [2005] concluded that for equal wave spectra at the toe of a coastal structure significantly more damage (order of 30%) occurs to a steep foreshore in contrast to a mild slope. By using the Morrison approach this difference in damage can be explained due to the increase in velocity and acceleration for waves travelling over a steep foreshore.

5.2 Recommendations

- Develop a method which increases the accuracy of measuring velocities and accelerations at the interface of the breakwater. In this way the relation between foreshore steepness and particle velocity and acceleration becomes clearer. Also the values can be used to do a study in a quantitative approach.
- Measure velocity and acceleration at the breakwater interface for a horizontal bed. The values can be compared with the used foreshore steepnesses.

- Check the behaviour of foreshore steepness and velocity and acceleration for breaking waves.
- Combine the velocity and accelerations measurements with actual damage tests. The combined data can lead to a stability parameter which includes the foreshore steepness.

References

Angremond, K. d' (2001) *Breakwaters and closure dams, Engineering the interface of soil and water part II*, Delft University Press, Delft, The Netherlands.

American Society of Civil Engineers (2000), *Manual on hydraulic modelling,* United States of America, Reston, Virginia.

Burcharth, H. F., Zhou, L., Troch, P. (1999). *Scaling of core material in rubble mound breakwater model tests.* Proc. 5th International Conference on Coastal and Port Engineering in Developing Countries, Cape Town, South Africa, pp. 1518-1528.

Coastal Engineering Manual, United States Army Corps of Engineers, 2003.

CUR Report 169, *Manual on the use of rock in hydraulical engineering*, Gouda, The Netherlands.

Dessens, M. (2004), *The influence of flow acceleration on stone stability,* M.Sc.Thesis, faculty of Civil Engineering, Delft University of Technology, Delft The Netherlands.

Drake, T.G. and Cataloni, J. (2001), Discrete particle mode for sheet flow sediment transport in the nearshore. Journal of geophy.Res.Oceans Vol. 106, No C9 pages 19.859-19.868.

Gent M.R.A van et al. (2003), *Stability of rock slopes with shallow foreshores*, Proc. Coastal Structures.

Goda, Y. (1985), *Random seas and design of maritime structures,* Advanced Series of Ocean Engineering, Volume 15.

Hovestad M. (2005), *Breakwaters on steep foreshores, the influence of the foreshore steepness on armour stability*, M.Sc.Thesis, faculty of Civil Engineering, Delft University of Technology, Delft, The Netherlands.

Schiereck, G.J. (2001), *Introduction to bed, bank and shore protection. Engineering the interface of soil and water part I*, Delft University Press. Delft, The Netherlands.

Tromp, M. (2004), *Influences of fluid accelerations on the threshold of motion*, M.Sc.Thesis, faculty of Civil Engineering, Delft University of Technology, Delft, The Netherlands.

Terrile, E., Reiniers, A., Stive, M.J.F., Verhagen, H.J. (2004), *incipient motion of coarse particles under regular shoaling waves.* Coastal Engineering Volume 53, pp 81-92.

Verhagen, H.J. (2005), *The effect of foreshore slope on breakwater stability*, ICS2005 Hövn, Iceland.

http://chl.erdc.usace.army.mil (website for download of Coastal Engineering Manual)

Appendix A

Calculation of the reflection of a regular wave

To calculate the reflection of a regular wave, a Matlab program Refreg has been written in the Laboratory of Fluid Mechanics. The method used has been described by Goda and Suzuki (1976), see Goda (1985). In this method two wave gauges are used at a distance of about one fourth of the wave length.

Basic equations in the case of a regular wave with wave gauges at positions $x=x_1$ en $x=x_2$ are:

$$\eta(x_1,t) = \sum_{n=1}^{N} a_{i,n} \cos\left(k_n x_1 - \omega_n t + \phi_{i,n}\right) + \sum_{n=1}^{N} a_{r,n} \cos\left(k_n x_1 + \omega_n t + \phi_{r,n}\right) \quad (1a)$$

$$\eta(x_2,t) = \sum_{n=1}^{N} a_{i,n} \cos\left(k_n x_2 - \omega_n t + \phi_{i,n}\right) + \sum_{n=1}^{N} a_{r,n} \cos\left(k_n x_2 + \omega_n t + \phi_{r,n}\right) \quad (1b)$$

η	the water-surface elevation relative to the mean water level
t	time
$a_{i,n}$, $a_{r,n}$	the amplitude of the n-th harmonic of the incoming and the reflected wave,
k_n	the wave number of the n-th harmonic,
ω_n	the angular wave frequency of the n-th harmonic,
$\phi_{i,n}$, $\phi_{r,n}$	the phase of the n-th harmonic of the incoming and the reflected wave.

In the Refreg program, the first harmonic is used only. Higher harmonic components and free or bound harmonics are not taken into account. Equations (1a) and (1b) for the first harmonic are

$$\eta(x_1,t) = a_i \cos\left(kx_1 - \omega t + \phi_i\right) + a_r \cos\left(kx_1 + \omega t + \phi_r\right) \quad (2a)$$

$$\eta(x_2,t) = a_i \cos\left(kx_2 - \omega t + \phi_i\right) + a_r \cos\left(kx_2 + \omega t + \phi_r\right) \quad (2b)$$

(2a) can be written as

$$\eta(x_1,t) = a_i \left\{\cos\left(kx_1 + \phi_i\right)\cos(\omega t) + \sin\left(kx_1 + \phi_i\right)\sin(\omega t)\right\} +$$

$$+ a_r\left\{\cos\left(kx_1 + \phi_r\right)\cos(\omega t) - \sin\left(kx_1 + \phi_r\right)\sin(\omega t)\right\}$$

or

$$\eta(x_1,t) = A_1 \cos(\omega t) + B_1 \sin(\omega t) \quad (3a)$$

In the same way, (2b) can be written as

$$\eta(x_2,t) = A_2 \cos(\omega t) + B_2 \sin(\omega t) \quad (3b)$$

$$A_1 = a_i \cos\left(kx_1 + \phi_i\right) + a_r \cos\left(kx_1 + \phi_r\right) \quad (4a)$$

$$B_1 = a_i \sin\left(kx_1 + \phi_i\right) - a_r \sin\left(kx_1 + \phi_r\right) \quad (4b)$$

$$A_2 = a_i \cos\left(kx_2 + \phi_i\right) + a_r \cos\left(kx_2 + \phi_r\right) \quad (4c)$$

$$B_2 = a_i \sin\left(kx_2 + \phi_i\right) - a_r \sin\left(kx_2 + \phi_r\right) \quad (4d)$$

(4a) through 4(d) lead to the complex equations:

$$A_1 + \mathrm{i}B_1 = a_i e^{\mathrm{i}kx_1} e^{\mathrm{i}\phi_i} + a_r e^{-\mathrm{i}kx_1} e^{-\mathrm{i}\phi_r} \quad (5a)$$

$$A_2 + \mathrm{i}B_2 = a_i e^{\mathrm{i}kx_2} e^{\mathrm{i}\phi_i} + a_r e^{-\mathrm{i}kx_2} e^{-\mathrm{i}\phi_r}, \quad (5b)$$

where i=√-1.

(5a) and (5b) can be written as matrices:

$$\begin{pmatrix} e^{\mathrm{i}kx_1} & e^{-\mathrm{i}kx_1} \\ e^{\mathrm{i}kx_2} & e^{-\mathrm{i}kx_2} \end{pmatrix} \begin{pmatrix} a_i e^{\mathrm{i}\phi_i} \\ a_r e^{-\mathrm{i}\phi_r} \end{pmatrix} = \begin{pmatrix} A_1 + \mathrm{i}B_1 \\ A_2 + \mathrm{i}B_2 \end{pmatrix} \quad (6)$$

The A and B in the right hand side of (6) can be found from a harmonic analysis of $\eta(x_1,t)$ and $\eta(x_2,t)$ in (3a) and (3b), e.g. by using a Fast Fourier Transform (FFT). In the program Refreg two zero crossings with the same sign, one at the begin and one at the end of the first data series, are used to determine the length of the series to be analysed. In that case the data series can be regarded as cyclic. The only error is a cut off error if the wave period does not fit on the time step. The FFT of Matlab is used on the two data series from the wave gauges under consideration, where the number of points used fits to the time between the zero crossings as meant above. The period with the maximum modulus of the FFT-coefficients is used as the base period.

calculating the amplitude and the phase of the incoming and the reflected wave

Equation (6) has the form L$\underline{a}$ = $\underline{b}$, where $\underline{a}$ and $\underline{b}$ are vectors and L is a matrix. This equation system can be solved in Matlab directly.

The wave number k is determined by the dispersion relation in case of free gravitation surface waves is used:

$$\omega = \sqrt{gk \tanh(kh)},$$

where ω is the angular frequency and g the gravitational acceleration constant. The calculation is performed by the Matlab-function Disper, written by Gert Klopman.

Transformatie van coördinatenstelsel

Het meten van punten vanaf een digitaal beeld of gedigitaliseerd beeld kan worden gedaan met het programma "scan_xy". Om uit de gemeten beeldpunten de werkelijke punten te berekenen moeten op het beeld enkele punten zichtbaar zijn waarvan de ligging t.o.v. het gewenste coördinatenstelsel bekend is. De opname moet in ieder geval planparallel zijn zodat er geen sprake is van perspectivische vertekening. Bij gebruik van het programma moeten 3 bekende punten zichtbaar zijn, de 3 punten bepalen een coördinatenstelsel waarvan O de oorsprong is. Het eerste punt is de oorsprong, het tweede punt (A) ligt op de x-as en het derde punt (B) ligt op de y-as. Meestal is beeld (de opname) enigszins verdraaid t.o.v. het coördinatenstelsel, verder is het beeld waarschijnlijk kleiner (of groter) dan de werkelijkheid en de punten in het beeld worden gemeten in pixels. De gemeten waarden worden getransformeerd naar het coördinatenstelsel van de werkelijkheid.

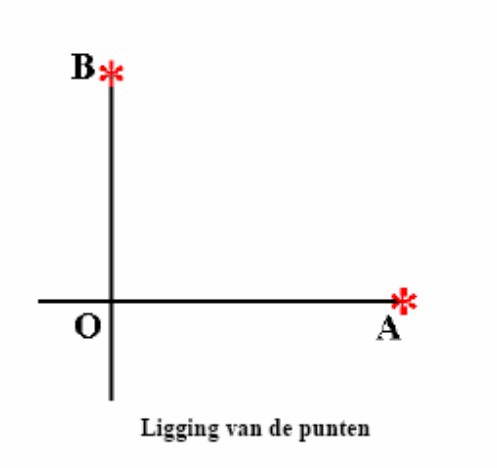

Ligging van de punten

Ligging van de punten
Het programma biedt ook de mogelijkheid voor uitvoer van de gemeten punten in beeldcoördinaten waarbij de waarden worden weergegeven in pixels.

Transformatie
De schalen van de x- en y-richting kunnen verschillen, in het bijzonder is dit het geval bij een opname gemaakt met een videocamera.

Parameters:
α : hoek waarover de camera is verdraaid
x' : schaalfactor in x-richting
y' : schaalfactor in y-richting

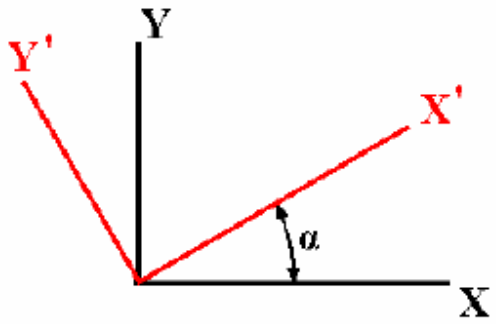

$$X' = s_x * (X * \cos(\alpha) + Y * \sin(\alpha))$$
$$Y' = s_y * (Y * \cos(\alpha) - X * \sin(\alpha))$$

Oplossing

<u>bepalen Sx en Sy</u>

$X_B = 0 \quad Y_A = 0$

$$X_A' = S_x * (X_A * \cos(\alpha) + Y_A * \sin(\alpha)) = S_x * X_A * \cos(\alpha)$$
$$X_B' = S_x * (X_B * \cos(\alpha) + Y_B * \sin(\alpha)) = S_x * Y_B * \sin(\alpha)$$
$$\frac{X_B'}{X_A'} = \frac{Y_B}{X_A} * \frac{\sin(\alpha)}{\cos(\alpha)} * \frac{S_x}{S_x} = \frac{Y_B}{X_A} * tg(\alpha) * 1$$
$$\alpha = \arctan(\frac{X_B'}{X_A'} / \frac{Y_B}{X_A})$$

$$X_A' = S_x * X_A * \cos(\alpha)$$
$$S_x = \frac{X_A'}{X_A * \cos(\alpha)}$$

$$Y_B' = S_y * (Y_B * \cos(\alpha) - X_B * \sin(\alpha)) = S_y * Y_B * \cos(\alpha)$$
$$S_y = \frac{Y_B'}{Y_B * \cos(\alpha)}$$

Bepaling van snelheden en versnellingen

De snelheden worden berekend uit een aantal opnamen met een digitale camera op tijdstippen met vaste tijdstap Δt. Hierin wordt de positie van een balletje in achtereenvolgende opnamen aangeklikt, en vervolgens opgeslagen. Het gebruikte programma is Multiscan_XY van Arie M. den Toom. Zie ook webpagina www.fluidmechanics.tudelft.nl , Laboratory, Support.

Voor het berekenen van snelheden en versnellingen is een Matlabscript Vels.m geschreven.

Aanwijzingen voor het gebruik:

Invoerbestand:

Invoer is het uitvoerbestand van Multiscan_xy. De algemene naam is Multiscanxy.dat. Om verschillende metingen te onderscheiden kan het zin hebben dit bestand een andere naam te geven.
Het invoerbestand bevat de volgende kolommen:

kolom 1: tijdindex bij de opname; bij index i hoort tijd i Δt,
kolom 2: volgnummer van de opname,
kolom 3: x-coördinaat van het aangeklikte punt in pixels,
kolom 4: y-coördinaat van het aangeklikte punt in pixels.

Onderaan het bestand staan de namen van de gebruikte bitmap-bestanden als invoer van Multiscan_xy.

Het programma Vels vraag het invoerbestand via een dialoogscherm. Beantwoord de vraag Read all samples? met no, en geef in het volgende scherm bij number of first sample to be read resp. number of last sample to be read de regelnummers van het eerste en het laatste te verwerken punt in het .dat-bestand. Deze komen i.h.a. overeen met de nummers in kolom 2 van dit bestand.

Invoergegevens:

Deze moeten worden opgeslagen in een parameterbestand naam.txt. Voor naam kan dezelfde naam worden gekozen als van het .dat-bestand.

Inhoud parameterbestand:

time step used: 0.0200
pos of origin [pixels]: 68 448
rightmost point of X-axes [pixels]: 627 461
uppermost point of Y-axes [pixels]: 71 205
rightmost point of X-axes [m]: 0.500 0.000
uppermost point of Y-axes [m]: 0.000 0.200
lower right endpoint of construction [m]: 0.560 0.000
upper left endpoint of construction [m]: 0.000 0.295

Hierin zijn de coördinaten in meter i.h.a. vast, behalve wanneer het referentiesysteem wordt verplaatst, of wanneer de constructie wordt gewijzigd.
De parameters worden opgeslagen in de volgende variabelen (in het programma zijn dit velden van een structure Inparm):

dt tijdstap tussen opeenvolgende beelden
pos0 [x y]: coördinaten van de oorsprong (snijpunt van twee op de wand aangebrachte lineaaltjes) in pixels,
pos1 [x y]: coördinaten van het eindpunt van de horizontale as (lineaal) in pixels,
pos2 [x y]: coördinaten van het eindpunt van de vertikale as (lineaal) in pixels.

De oorsprong wordt geconverteerd naar [0 0]. De eindpunten moeten worden opgegeven:
new1 [x y]: coördinaten van het eindpunt van de horizontale as (lineaal) in m; op dit moment is dat [0.5 0],
new2 [x y]: coördinaten van het eindpunt van de vertikale as (lineaal) in m; op dit moment is dat [0 0.2].

Verder moeten de eindpunten van de constructie worden opgegeven:
x1 [x y]: coördinaten van het eindpunt rechtsonder in de constructie in m (in oudere versies: pixels,
x2 [x y]: coördinaten van het eindpunt linksboven in de constructie in m (in oudere versies: pixels).

Opm.: in oudere versies werden deze gegevens handmatig ingevoerd in Vels.m. Zie ook: Vels8.m.

Coördinatentransformatie naar de gegeven assen (incl. omrekenen van pixels naar m):

Alle gegeven coördinaten zijn opgeslagen na aanklikken in een afbeelding van het bitmap-bestand (programma Multiscan_xy). Hierin zit enige spreiding, waardoor de gegeven assen (punten van de lineaals) niet precies loodrecht op elkaar staan. Hiervoor wordt niet gecorrigeerd. Er wordt van uitgegaan dat in alle coördinaten een soortgelijke spreiding zit.
De transformatiematrix At wordt direct berekend uit de gegeven coördinaten:

[new1 ' new2 '] = At * [(pos1 - pos0)' (pos2 - pos0)'] (1)

In dit geval volgt At uit:

At = [new1 ' new2 '] / [(pos1 - pos0)' (pos2 - pos0)'] (2)

(zie "Using Matlab Version 6", paragraaf 11, p. 11-13 e.v.: "Solving Linear Equations").

De kolommen van de matrix [new1 ' new2 '] in (1) en (2) zijn de coödinaten van de punten op de gegeven (nieuwe) assen in m; de kolommen van [(pos1 - pos0)' (pos2 - pos0)'] zijn de coördinaten van de punten op de gegeven assen in het oude coördinatenstelsel (camera) t.o.v. de nieuwe oorsprong.
Als een willerkeurig paar coördinaten (x_i ,y_i) in pixels is gegeven volgen de coördinaten (($x_n)_i$,$y_{n)i}$)) in meter t.o.v. de nieuwe assen uit:

$$\begin{bmatrix} (x_n)_i \\ (y_n)_i \end{bmatrix} = At \begin{bmatrix} x_i - pos0(1) \\ y_i - pos0(2) \end{bmatrix} \qquad (3)$$

4. Bepaling van de snelheden:

Het invoerbestand wordt ingelezen in een matrix A, waarvan de kolommen overeenkomen met de kolommen in het invoerbestand. Sommige punten in het invoerbestand zijn geen coördinaten van het balletje. Deze punten liggen meestal buiten het bereik [thresh, thresh], waarbij thresh een te kiezen drempel is (in pixels). Voorlopig is in de x- en y-richting dezelfde drempel gekozen, met voorlopige waarde 100. De drempel kan worden aangepast door editen van de functie FN_velsn.m. Hierbij is n een versienummer. Welke versie van FN_vels wordt gebruikt kan worden nagegeaan in het hoofdprogramma Vels.m.
In het uitvoerbestand naam.txt (zie punt 7.) worden de weggelaten punten met een * aangegeven.
Na weglaten van de punten buiten het bereik worden de tijden in seconden berekend, en de coördinaten omgezet van pixels naar meters m.b.v. vergelijking (3). De nieuwe tijden komen in matrix A1, die is onstaan uit A na weglating van de punten buiten het bereik. Voor de verdere berekening bleek het handig de nieuwe coördinaten van de posities op te slaan in een aparte matrix B.
De snelheden moeten nu worden geschat door numerieke differentiatie van de posities. Omdat bij het bepalen van differenties de in het signaal aanwezige fluctuaties worden versterkt wordt eerst een glijdend gemiddelde over 3 punten uitgevoerd. Hiervoor is de Matlabfunctie filtfilt gebruikt, waarin het middelingsproces in twee richtingen wordt uitgevoerd. Op die manier treedt geen faseverschuiving op (zie fig. 1). In een test bleek dit een beter resultaat te geven dan de functie filter, waarbij in één richting wordt gemiddeld.

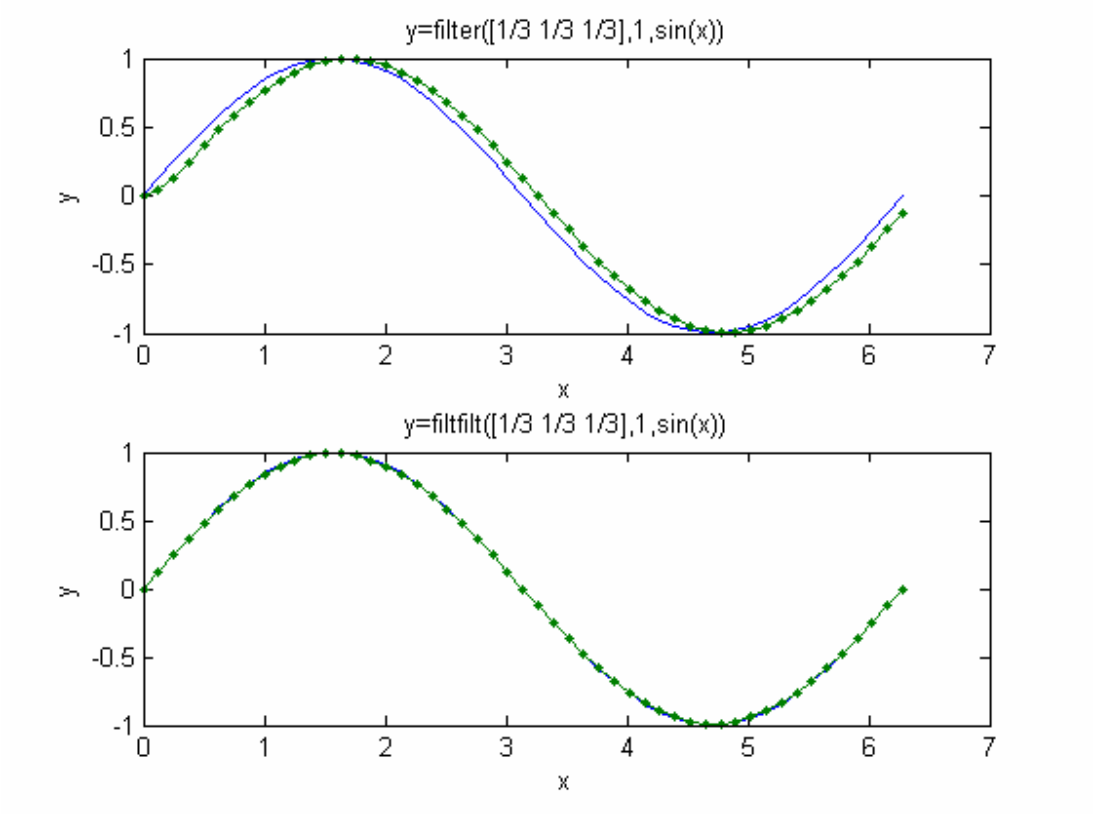

fig. 1: glijdend gemiddelde over 3 punten met resp filter en filtfilt

De numerieke differentiatie wordt uitgevoerd over het glijdend gemiddelde van de posities met bijbehorende tijden. Dit gebeurt met de Matlabfunctie diff, waarbij centrale differenties ontstaan voor punten tussen de monsterpunten. De bijbehorende tijden en coördinaten worden berekend door lineaire interpolatie tussen de puntenparen.

Bepaling van de versnellingen:

Deze worden berekend uit differenties van de snelheden en de bijbehorende tijden. De snelheden worden ook weer vooraf "gemiddeld" over drie opeenvolgende punten met filtfilt. Na numerieke differentiatie worden de bijbehorende tijden en plaatscoördinaten worden weer tussen elk puntenpaar genomen.

Berekening van de componenten t.o.v. de constructie

De componenten van snelheden en versnellingen t.o.v. de constructie worden berekend uit de opgegeven coördinaten van de constructie. Dit levert een nieuwe transformatiematrix.

Uitvoer:

Uitgevoerd worden:
Een vectorplot van resp. snelheden en versnellingen, met de bijbehorende constructie als ingetekende lijn.

Een bestand naam.txt met afdruk van de invoerparameters, de berekende transformatie-matrices (naar gegeven assen, en vervolgens van assen naar constructie), en de meetgegevens met markering van de weggelaten punten. Naam is een door de gebruiker te kiezen naam; het pad wordt gekozen via een dialoogscherm.

Een bestand naam.asc met berekende snelheden en versnellingen. De kolommen bevatten achtereenvolgens:

glijdend gemiddelde over 3 punten van de tijd in s
glijdend gemiddelde over 3 punten van de x-coördinaat in m
glijdend gemiddelde over 3 punten van de y-coördinaat in m
$sign(ucL)\sqrt{ux^2 + uy^2}$ in m/s, resp. $sign(acL)\sqrt{ax^2 + ay^2}$ in m/s^2
ux: x-component snelheid, resp. ax: x-component versnelling
uy: y-component snelheid, resp. ay: y-component versnelling
ucL: snelheidscomponent in de richting van de constructie,
resp. acL: versnellingscomponent in de richting van de constructie,
ucn: snelheidscomponent loodrecht op de constructie,
resp. acn: versnellingscomponent loodrecht op de constructie.

Opm: de hier opgeslagen snelheden en versnellingen zijn na het differentiatieproces niet gemiddeld.

Middelen van de afgeleide i.p.v. bepaling van de afgeleide van het gemiddelde

Van het programma Vels is ook een oudere versie Vels5a beschikbaar (a: met invoer nieuwe stijl), waarbij de snelheden door numerieke differentiatie van de niet gefilterde posities worden

bepaald, en vervolgens gemiddeld. Een bezwaar hierbij kan zijn dat in het signaal aanwezige fouten bij de numerieke differentiatie kunnen worden versterkt, doordat het aantal significante cijfers kleiner wordt. Dit effect is bij filteren vooraf kleiner.

	Foreshore steepness	$\overline{U}_{\max;neg}$ [m/s]	$\overline{U}_{\max;pos}$ [m/s]	SD($\overline{U}_{\max;tot}$) [m/s]	SD($\overline{U}_{\max;tot}$) [m/s]
s3H6	1:08	-0,68	0,77	0,17	0,12
	1:15	-0,56	0,62	0,04	0,04
	1:30	-0,50	0,59	0,07	0,04
s3H8	1:08	-0,71	0,74	0,07	0,05
	1:15	-0,59	0,69	0,10	0,07
	1:30	-0,65	0,77	0,13	0,09
s3H10	1:08	-0,69	0,77	0,07	0,07
	1:15	-0,71	0,76	0,09	0,06
	1:30	-0,75	0,83	0,14	0,09
s4H6	1:08	-0,63	0,65	0,10	0,07
	1:15	-0,60	0,61	0,06	0,05
	1:30	-0,53	0,57	0,08	0,06
s4H8	1:08	-0,77	0,78	0,12	0,07
	1:15	-0,71	0,73	0,11	0,06
	1:30	-0,63	0,72	0,05	0,10
s4H10	1:08	-0,86	0,90	0,13	0,09
	1:15	-0,74	0,79	0,14	0,09
	1:30	-0,85	0,74	0,21	0,08
s4H12	1:08	-0,96	0,99	0,18	0,14
	1:15	-1,18	0,92	0,24	0,19
	1:30	-0,95	0,98	0,16	0,08
s6H8	1:08	-0,64	0,65	0,06	0,07
	1:15	-0,69	0,62	0,12	0,10
	1:30	-0,67	0,64	0,16	0,09
s6H10	1:08	-0,77	0,80	0,12	0,08
	1:15	-0,77	0,75	0,14	0,08
	1:30	-0,78	0,78	0,15	0,09
s6H12	1:08	-0,90	0,87	0,25	0,12
	1:15	-0,88	0,81	0,28	0,19
	1:30	-0,89	0,83	0,20	0,09

table C.1: Mean maximum velocities and standard deviations, measured at the breakwater slope.

	Foreshore steepness	$\overline{A}_{max;\,pos}$ [m/s^2]	SD($\overline{A}_{max;\,pos}$) [m/s^2]	$\overline{A}_{max;neg}$ [m/s^2]	SD($\overline{A}_{max;neg}$) [m/s^2]
s3h6	1:8	2,75	0,75	-4,27	1,84
	1:15	2,10	0,32	-3,89	2,20
	1:30	2,36	0,82	-2,83	2,27
s3h8	1:8	3,18	0,45	-4,43	1,99
	1:15	2,13	0,48	-4,10	2,14
	1:30	2,72	0,94	-4,19	2,55
s3h10	1:8	2,50	0,39	-4,29	2,54
	1:15	2,70	0,72	-3,16	1,77
	1:30	2,76	0,43	-3,46	1,78
s4h6	1:8	2,48	0,27	-3,93	0,46
	1:15	2,45	0,27	-4,30	0,43
	1:30	2,37	0,29	-3,94	0,51
s4h8	1:8	2,95	0,49	-5,44	0,68
	1:15	2,54	0,41	-5,05	0,75
	1:30	2,84	0,68	-4,30	1,98
s4h10	1:8	3,70	0,58	-6,00	0,72
	1:15	2,48	0,31	-3,76	2,73
	1:30	3,55	0,42	-5,90	1,01
s4h12	1:8	3,75	0,36	-6,96	0,23
	1:15	3,20	0,76	-5,83	1,83
	1:30	3,77	0,44	5,36	1,22
s6h8	1:8	2,83	0,43	-5,07	0,29
	1:15	2,84	0,45	-5,10	0,64
	1:30	3,02	0,49	-5,09	0,61
s6h10	1:8	3,43	0,04	-6,30	0,09
	1:15	2,91	0,28	-5,55	0,87
	1:30	3,28	0,41	-5,81	0,54
s6h12	1:8	4,21	0,38	-6,90	0,56
	1:15	3,34	0,39	-6,37	0,72
	1:30	3,54	0,29	-6,31	0,50

tableC.2 Mean maximum acceleratons (7-point averaged) and standard deviations, measured at the breakwater slope.

The derivation of $\frac{gH_T T^2}{L_T^2} \propto \frac{H_T}{H_B}$ is given as follows:

$L_0 = \frac{gT^2}{2\pi}$ so $gT^2 = 2\pi L_0$ by substitutions follows $\frac{2\pi H_T L_0}{L_T^2}$

from the linear wave theory the dispersion relation is known:

$\omega^2 = gk\tanh(hk)$ by substituting $\omega = \frac{2\pi}{T}$ and $k = \frac{2\pi}{L}$ the shallow water wave length is

given by the following equation

$L = L_0 \tanh(hk)$ thus $\tanh(hk) = \frac{L}{L_0}$

The theory of Miche implies that the maximum wave height is limited by the wave steepness. The formula concludes:

$H_B \cong 0.14L\tanh(kh)$ so $\frac{H_B}{L} \cong 0.14\tanh(kh)$ by substitution follows

$\frac{H_B}{L} \cong 0.14\frac{L}{L_0}$ thus $\frac{L_0}{L^2} \cong \frac{0.142}{H_B}$ substituting this in the original formula gives the relation to the dimensionless breaker height:

$\frac{2\pi H_T L_0}{L_T^2} \cong \frac{2\pi \cdot 0.142 \cdot H_T}{H_B} \propto \frac{H_T}{H_B}$